Estimating the size at maturity of fishes from stereo-video surveys of fish spawning aggregations

Steven Lindfield, Coral Reef Research Foundation
Patrick Colin, Coral Reef Research Foundation
John Swords, Coral Reef Research Foundation
Brett Taylor, Australian Institute of Marine Science
Jeremy Prince, Biospherics, Pty Ltd

Correspondence: steve.lindfield@gmail.com

Table of Contents

Executive summary

This study was the first to estimate fish size at maturity of aggregation spawning fishes using underwater stereo-video. By sampling twelve species of fish that form spawning aggregations using a diver-operated stereo-video system (8860 length measurements) and concurrently dissecting fish from fish markets over a 24 month period (1325 samples), we were able to generate reliable size at maturity (length at 50% maturity; L_{50}) values which were consistently correlated with the far left-hand side of spawning aggregation length frequency distributions. Using these techniques, we were able to generate an average probability density value from the length frequency distribution of spawning aggregations, which can then be used predict size at maturity (L_{50}) values with confidence intervals from other length frequencies. The use of this average probability density was then used on an additional six species of reef fish that were measured by stereo-video in spawning aggregations in order to predict their size at maturity. This framework provides a novel cost-effective methodology to estimate size at maturity in a non-destructive way as fish do not need to be captured or dissected. These findings also have application for expanding this method across other coral reef locations to cost effectively compare the variation in life-history values across geographic gradients using a standardized technique. These newly estimated size at maturity values are further used to update data-poor stock assessments in Palau and provide robust data for the implementation of minimum size limits as an effective fisheries management tool.

Introduction

The size at which fish become adult is one of the most fundamental aspects of fisheries biology (Brown-Peterson et al. 2011; Flores et al. 2015). Referred to variously, but not exclusively, as size of/at maturity, maturation occurs across a size range commonly described with a logistic function using L_{50} and L_{95}, to represent the length classes in which 50% and 95% of individuals have attained adulthood respectively. Standard techniques for estimating size at maturity involve dissecting large samples of fish across their size range so that gonads can be examined and classified either macroscopically (from visual assessment) or microscopically (from histology slides).

Although the size at maturity is one of the cheapest forms of biological data widely used for stock assessments, for small scale fisheries, these size at maturity studies can still be prohibitively expensive and logistically challenging to collect. In the context of coral reef fisheries, more than 100 species may be landed (Prince et al. 2018). Samples of each species need to be obtained a few at a time throughout the year from small local markets. Fishing bans through spawning season may prevent sampling when gonadal classification is simplest and size selective bias in catches can limit the sampling of juvenile size classes, making L_{50} estimation impossible without focused fishing to target juveniles. Many small Pacific island nations do not have the budget, expertise or facilities to conduct these studies, and even though

size at maturity varies considerably across a species' range with water temperature and latitude (Robertson et al. 2005; Trip et al. 2008; Taylor et al. 2019), size at maturity estimates from other countries are commonly used which can lead to inaccuracies when assessing stock status.

To help sustain the world's fisheries, there is a need to develop simple data-driven management policies that are understood by all stakeholders. With this recognition, data-poor stock assessment techniques have been developed to help bridge the gap between the expensive data-rich assessments conducted only for the most valuable fisheries in the world, and the vast majority of smaller fisheries, especially those on coral reefs that support millions of fishers. By some estimates, 90% of the world's fisheries, which directly support 14 - 40 million fishers and indirectly support approximately 200 million people, are un-assessable with conventional methods (Andrew et al. 2007). Therefore, there has been a great interest in developing data-poor stock assessment methods in recent years, which are typically based on the size structure of the population (Hordyk et al. 2015; Nadon et al. 2015).

Data-poor stock assessment techniques such as length-based assessments of spawning potential ratio (LB-SPR) require life-history ratios of natural mortality to growth rate (M/k) and the length at maturity to asymptotic length (L_m/L_∞), along with the size frequency structure of the population, and an estimate of local size at maturity and or asymptotic length (Prince et al. 2015b; Hordyk et al. 2015). It is through these input parameters that the spawning potential ratio (SPR), a widely used reference point for fishery stock assessments, can be estimated. Even though the life-history ratios of (M/k) and (L_m/L_∞) are relatively stable geographically and between species when compared to the individual parameters (Prince et al. 2015a), robust assessments still require a local size at maturity, or asymptotic length, for each species. Gathering data on asymptotic length can be difficult to impossible in heavily fished populations, where the largest fishes have already been removed. Size at maturity on the other hand is thought to be less impacted by fishing pressure, and although it can be costly and time consuming to collect, it provides a vital parameter for data-poor stock assessments and is necessary to set biologically meaningful size limits that can preserve minimum SPR reference points when managing a fishery with limited data and resources.

Many of the most important subsistence and commercially valuable reef fishes aggregate in large numbers at specific times and places to reproduce (Colin 2012a). These fish spawning aggregations provide a unique window where the numbers of fish are at greatly elevated densities and where it is presumed only reproductively active fish are present. Aggregations can be defined in two types; 1) Resident spawning aggregations, where individuals from a relatively small and local area spawn regularly (often daily) for relatively shorter periods of time (i.e., hours); and 2) Transient aggregations, where individuals travel greater distances to form aggregations that often do not form all year round but persist for longer (days), and often have a lunar component (Domeier & Colin 1997). It is increasingly recognized that fish spawning aggregations should be a focal point for fisheries management and conservation on a global scale, with a particular emphasis placed on the protection of transient spawning aggregation sites (Erisman et al. 2015). Both types

of spawning aggregation sites can serve as scientific platforms for monitoring population trends. We propose that they can also provide valuable, non-detrimental access to life-history parameters needed for stock assessments and management initiatives such as size limits.

With improvements in underwater stereo-video photogrammetry, it is possible to accurately measure fish lengths non-invasively (Shortis et al. 2009). These stereo-video systems can therefore greatly improve the statistical power to detect changes in size structure compared to visual estimates (Harvey et al. 2002). Along with constantly improving high-definition video cameras and specialized software used to analyse stereo-video footage, diver operated stereo-video systems provide an accurate and effective method for fishery-independent surveys of fishes (Goetze et al. 2019).

Previous approaches used to estimate the length at maturity in Palau for LB-SPR assessments (Prince et al. 2015b) was to train collaborating fishers in the macroscopic (visual) examination of fish gonads, and rely on larger sample sizes to fit logistic curves to estimate the length at which 50% maturity occurs. However, given the complexity of categorizing the developmental stages of tropical fish, the truncated nature of size structures, and the relatively low level of training provided to the collaborating fishers, the size at maturity data collected in this way are sparse and very noisy for most species. Even when experienced scientists perform macroscopic inspections and staging classifications, they are known to misclassify reproductive parameters, typically by overestimating the proportion of mature individuals (Vitale et al. 2006; Longenecker et al. 2013). To avoid such errors, histological studies are recommended as the most accurate methodology to determine an individual's stage of sexual maturation (West 1990; Brown-Peterson et al. 2011; Flores et al. 2015).

Project goals

The goal of this study was to improve the cost effectiveness and accuracy of generating size at maturity (L_{50}) values by providing an alternative to the fishery-dependent dissection and examination of fish gonads. By using a fishery-independent method of sampling of spawning aggregations with diver operated stereo-video, we aim to develop a technique to non-destructively estimate size at maturity and also improve the cost effectiveness for generating these values. Then using new size at maturity values, we can update data-poor stock assessments and provide fishery management recommendations. This goal is addressed through the following four objectives:

1) Use stereo-video to sample the size of aggregating coral reef fishes that are targeted by fishing, and sample at multiple sites and times during the year for each species of interest.

2) Fishes that can be successfully sampled for size frequencies with stereo-video will be sampled from fisher catches to examine gonadal maturity and estimate a value for length at 50% maturity.

3) Compare the size at maturity to the length frequency data generated from the stereo-video data for the different species to validate any consistent relationships between the two techniques.

4) Use the new maturity estimates to refine data-poor stock assessments and work with fishers, markets, managers and agencies to propose updated size limits for species where this information was previously lacking.

Methods

Fishery-independent data collection of size frequencies at fish spawning aggregations

To sample the size structure of the aggregations we used a diver operated stereo-video system (stereo-DOV) (Goetze et al. 2019). Stereo-video systems consist of two high definition video cameras in underwater housings separated on a base bar and converged at a set angle (Figure 1). Through this, fish length and orientation can be measured in 3 dimensions, thereby providing highly accurate and precise measurements of fish size (Harvey et al. 2010). The software, EventMeasure–Stereo (www.seagis.com.au/event.html) was used for the post processing of stereo-video footage (Figure 2). This software can output a list of lengths in a text file which can be imported into statistical or graphing packages for analysis.
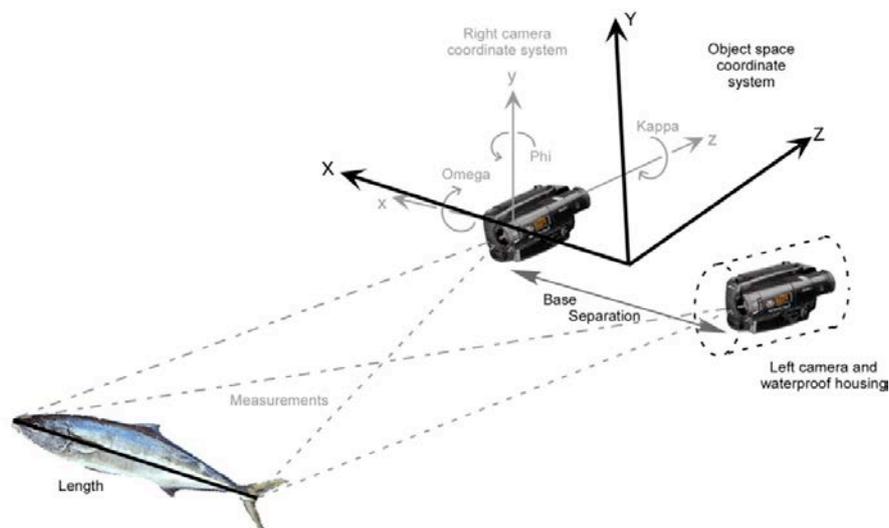
Figure 1: Schematic view of a stereo-image coordinate system and measurement of a length from 3-dimensional coordinates (reproduced from Shortis et al. 2009).
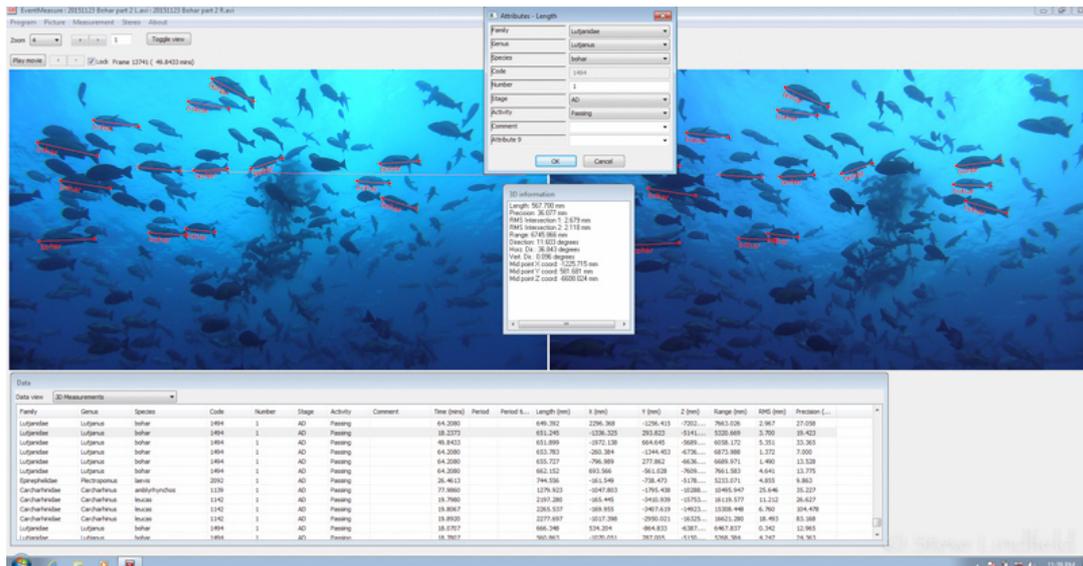
Figure 2: Screenshot showing the use of EventMeasure-Stereo to gather length data at an aggregation of *Lutjanus bohar* in Palau.

This study was based in Palau where there is a long history of fisher knowledge regarding spawning aggregations, scuba diving tourism that frequent known aggregation sites and detailed scientific surveys focused on fish spawning aggregations. The book 'Words of the Lagoon' (Johannes 1981) describes in detail the reproductive rhythms and spawning locations as understood from fisher knowledge. Based on fisher interviews, Sadovy (2007) also reported on the current status and exploitation history of reef fish spawning aggregations in Palau. Based on diving observations, published scientific information covers multiple species of grouper (Johannes 1999; Sadovy de Mitcheson et al. 2020), snapper (Sadovy de Mitcheson et al. 2012; Sakaue et al. 2016), parrotfishes (Colin 2012b), wrasse (Colin 2010), trevallies (Colin 2012c), moorish idols and unicornfish (Etpison & Colin 2018). Some of the known locations of spawning aggregations are presented in Figure 3.
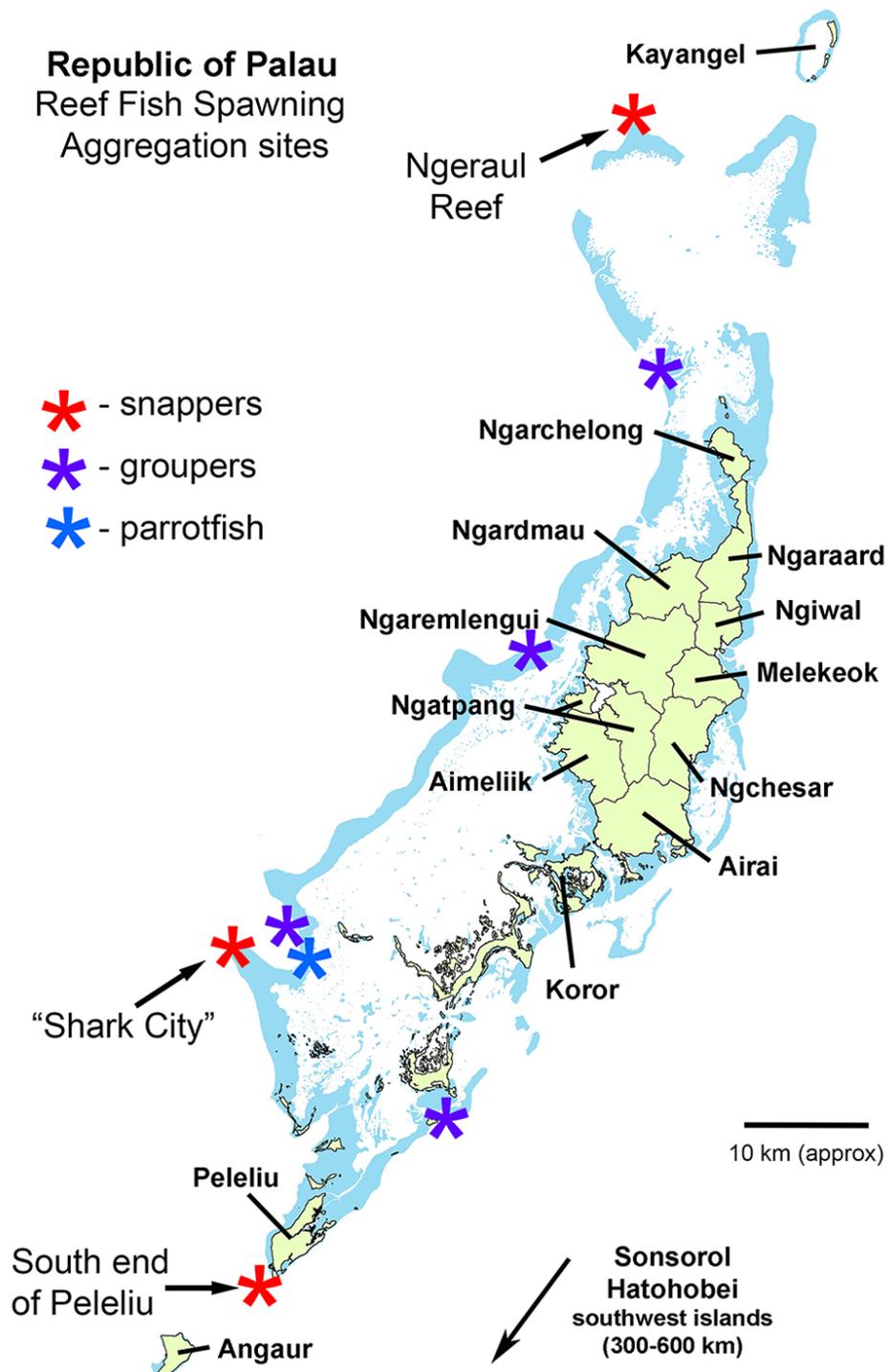
Figure 3: Location of some of main fish spawning aggregations in Palau

To increase the relevance of this work to other locations, we also sampled a grouper spawning aggregation in Pohnpei, Federated States of Micronesia (Rhodes et al. 2013, 2014). During, 5 days diving in April 2019 we sampled 262 *Plectropomus areolatus* grouper from two different aggregation sites, Kephera and Ahnd Atoll.

Figure 4: Images of the primary investigator with stereo-video camera and DSLR camera for recording aggregations. Diving is done using a closed-circuit rebreather which does not produce bubbles and allows closer approach to the fish. Photos by Niall McCarty.

To record aggregations, we used a combination of diving with a stereo-video system and also using high resolution DSLR camera to photograph fish schools. In addition, remote time-lapse cameras were used to document aggregations in the attempt to confirm spawning without the presence of divers. The majority of fish forming aggregations can be approached by normal scuba diving, however to maximize the limits of no-decompression dive time and to not disturb the fish, a closed circuit rebreather was used for diving as it does not produce bubbles and allows a closer approach to the fish for more accurate measurements (Lindfield et al. 2014). Filming using the stereo-video camera was done in a way as to avoid duplicate recordings of individual fish on a given day. For some species such as grouper that are distributed over a wide area and stay relatively stationary, the length of the site was surveyed slowly in one direction pointing the camera at each individual fish seen. Whereas for other fish such as the snappers that form aggregations of 1000s of fish which are actively swimming around, the diver aimed to position themself in a location where a wall of fish would swim past while remaining relatively stationary.

Biological sampling and histological processing

For species that were possible to film with stereo-video camera in a spawning aggregation, we aimed to collect at least 100 individual fish from fish markets in Palau for biological sampling. Sampling of fish focused on obtaining an evenly distributed length classes from the smallest to largest fish possible, sampling a few fish regularly during the first 2 years of the project (Sept 2017 to August 2019) during different moon phases and focused sampling at times of known spawning aggregation formation. Some species were easily to obtain, but others were rarely landed. For other species, finding immature fish was difficult and we needed supplement fish market sampling with focused spearfishing for small individuals. The majority of fish were purchased from the JR5 market in Koror, Palau, and some were also bought at the Surangels supermarket and the Northern Reef Fisheries Cooperative.

The processing took place at the Coral Reef Research Foundation and a protocol was developed to assure data quality and minimize the potential mislabelling of samples. The steps involved in processing the samples were as follows:

- Whole fish samples were kept on ice and processed the same day where possible, only fresh fish (not frozen) were sampled for histological processing.
- Each fish was tagged with a unique code (such as LO_001) using a cable tie through the gills and mouth (Figure 5a), measured for length (fork length and total length) and weighed to the nearest gram on electronic scales (Figure 5b). The data being recorded on a waterproof data sheet.
- The body cavity of the fish was then opened by placing a knife in the vent and running towards the underside of the head (Figure 5c). The gonads (testes or ovaries) were carefully separated from the other parts of the body cavity and fatty deposits trimmed away while maintaining the gonad's attachment to the vent.
- Once gonads had been dissected out of all the fish, the fish were placed on the table in numerical order and small tags with each fish's unique code placed above the open body cavity (Figure 5d).
- These fish were then filmed with a 3D camera – Fujifilm 3DW3 - (which can allow post processing of lengths if a mistake was made when measuring with the ruler) then individual fish were photographed with the camera taking 3D images (which provided better quality resolution compared to the video). Macro photographs were taken of each fish gonad while attached to the fish (Figure 5e).
- After photographing the fish, each gonad was examined visually (macroscopically) and preliminarily classed as being male or female and either immature or mature.
- Each gonad (both lobes) were then removed from the fish and placed in a sample tube (size depending on size of gonad) along with the sample label

(Figure 5f). The weight of each gonad sample was taken to the nearest 0.01 gram by zeroing the scale to the weight of the sample jar. Gonad weights were recorded on data sheet.

- The sample jar was then filled with 10% formalin seawater and stored for later histological processing, aiming to have at least a 5:1 formalin to gonad ratio. If the gonad was large, then it was sliced first to help the penetration of formalin for preservation.

- Although not needed for this study of size at maturity, we also utilized the fish samples to collect other valuable biological data, often at a later date after freezing the heads. The ear bones (otoliths) were removed from the head of the fish, cleaned in alcohol and stored dry. A small clip of the fin was stored in 95% ethanol for genetic analysis, and a sample of flesh collected from each fish and frozen for stable isotope analysis. These samples may be analysed at a later date or contributed to collaborations with other scientists working on these species. These samples are stored at the Coral Reef Research Foundation in Palau.

- When ready for histological processing (normally with a sample size of ~ 250 across all species), the gonads were removed from the formalin and a cross section though the middle of one gonad lobe (~4 mm thick) sliced off with a cleaned scalpel/razor blade. If the gonad was <25mm wide the cut sampled the whole cross section of the gonad, otherwise a half or 'pie slice' of the gonad was removed, keeping part of the gonad wall. The sample was placed in a histology cassette and labelled with the sample number and placed in a 'whirl pack' bag, typically 12 per pack and sealed with ~ 10 ml of formalin inside to keep the samples moist. These samples were then sent to the University of Hawaii, John A. Burns School of Medicine, Histopathology Core Facility or the Clinical Labs of Hawaii.

- The samples were returned to the Coral Reef Research Foundation on microscope slides having been sectioned transversely at 6 mm and stained with haematoxylin and eosin.

- These microscope slides were viewed under a compound microscope with digital camera connected to a computer monitor. There the gonads were classified as male or female and classified by developmental stages using the standardised terminology described by Brown-Peterson et al. (2011) in their Tables 2 & 3, which we present here below as Tables 1 & 2.
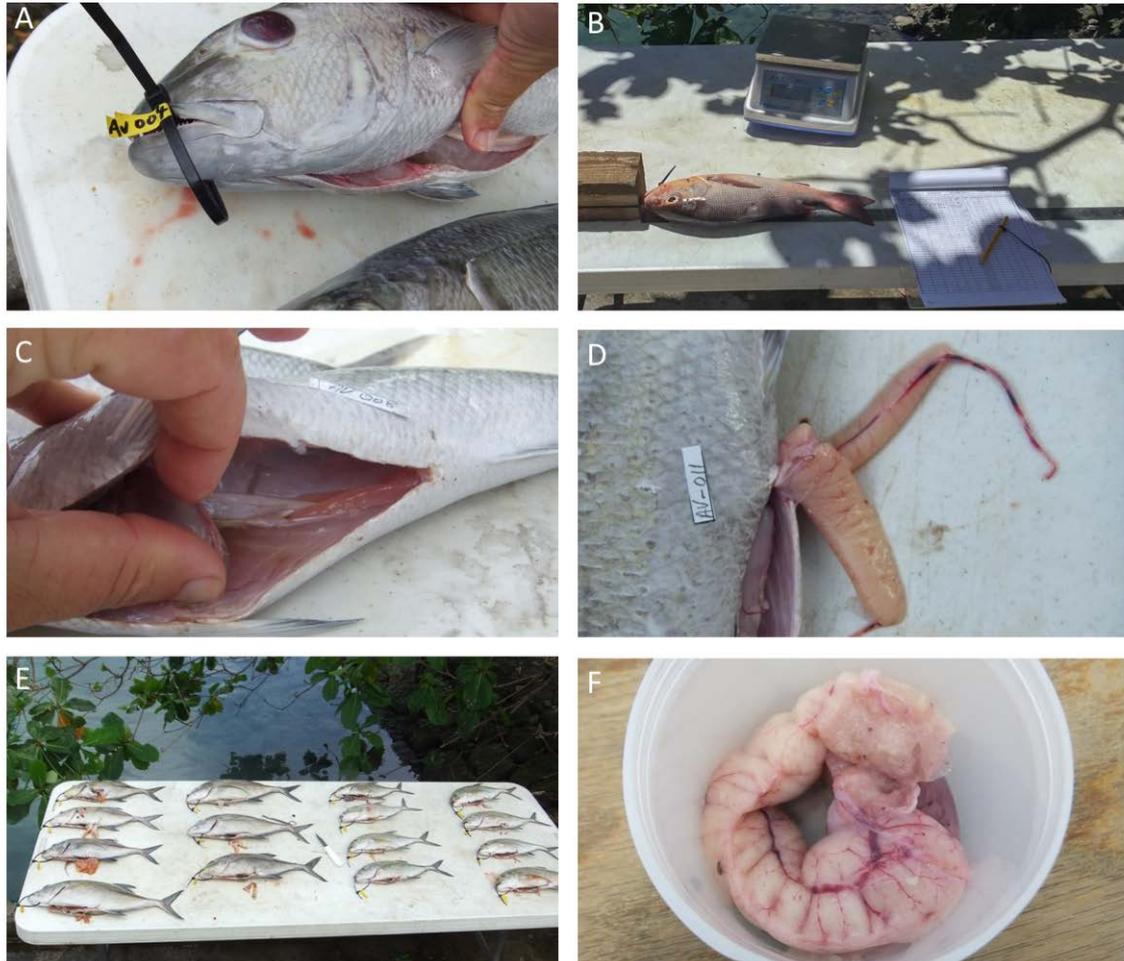
Figure 5: Images of steps during biological sampling.

Gonad classification

Aiming to standardize the classification of histological samples, Brown-Peterson et al. (2011) developed a universal terminology describing key phases of the reproductive cycles fishes that can be identified by specific histological and physiological markers independently of temporal aspects of gamete development. In the immature phase, gonadal differentiation as well as gamete proliferation and growth is gonadotropin independent. Maturity begins with an initial 'developing phase' marked by the commencement of gonadotropin-dependent gonad development that may take longer than one year, during which no gametes are released (Junquera et al. 2003; Brown-Peterson et al. 2011). During the second phase of maturity, gamete development advances sufficiently to allow for spawning within the current reproductive cycle, in females the leading cohort of gametes reach third stage vitellogenesis, and spermatozoa are present in the lumen of the lobules in males. At this stage individuals are 'spawning capable' and may enter the actively spawning subphase, during which hydration and ovulation occurs in females, and spermiation in males. The end of the reproductive cycle is indicated by

12

the regressing phase which is then followed by the regeneration phase before moving back into the developing phase to begin the cycle again.

While adopting Brown-Peterson et al.'s (2011) terminology, recent studies of Indo-Pacific reef fish (DeMartini et al. 2014; Taylor et al. 2016, 2018) have essentially regarded Brown-Peterson et al.'s (2011) 'developing phase' as being the terminal phase of juvenile life, rather than the initial phase of maturity if there are no signs of previous spawning. Using their classification, immature virgin developing female fish may have primary vitellogenic oocytes and it is not until oocytes have progressed to later vitellogenic stages when they are classified as mature. With regard to males, Brown-Peterson et al. (2011) define any spermatogenesis more advanced than primary spermatogonial proliferation as mature, whereas the criteria used more widely for coastal fishes regard males as mature only when there is active spermatogenesis in sperm crypts and tailed spermatozoa are present in tubules/lobules of testes (Murphy & Taylor 1990; Marriott et al. 2007).

We therefore chose to adopt a classification scheme where we regard the 'developing' phase defined by Brown-Peterson et al. (2011) as being immature if there are no signs of previous spawning. However, if there are signs of previous spawning such as those used the characterize the 'regenerating' phase such as muscle bundles, thick ovarian wall and atretic delta or gamma stage oocytes (Table 1), then we termed these fish belonging to an additional phase called 'redeveloping' which is regarded as mature. To compare variation that may be attributed to these different classification schemes, we also present size at maturity estimates derived by following the unmodified Brown-Peterson et al. (2011)'s classification scheme for which we call 'standardised' estimates.

Table 1. Standardised terminology for the histological classification of female fish gonads as described by Brown-Peterson et al. (2011) in their Table 2 and used by this study.

TABLE 2. Macroscopic and microscopic descriptions of the phases in the reproductive cycle of female fishes. Timing within each phase is species dependent. Some criteria listed for phases may vary depending on species, reproductive strategy, or water temperature. Subphases that apply to all fishes are listed; additional subphases can be defined by individual researchers (CA = cortical alveolar; GVBD = germinal vesicle breakdown; GVM = germinal vesicle migration; OM = oocyte maturation; PG = primary growth; POF = postovulatory follicle complex; Vtg1 = primary vitellogenic; Vtg2 = secondary vitellogenic; Vtg3 = tertiary vitellogenic).

Phase	Previous terminology	Macroscopic and histological features
Immature (never spawned)	Immature, virgin	Small ovaries, often clear, blood vessels indistinct. Only oogonia and PG oocytes present. No atresia or muscle bundles. Thin ovarian wall and little space between oocytes.
Developing (ovaries beginning to develop, but not ready to spawn)	Maturing, early developing, early maturation, mid-maturation, ripening, previtellogenic	Enlarging ovaries, blood vessels becoming more distinct. PG, CA, Vtg1, and Vtg2 oocytes present. No evidence of POFs or Vtg3 oocytes. Some atresia can be present. *Early developing subphase*: PG and CA oocytes only.
Spawning capable (fish are developmentally and physiologically able to spawn in this cycle)	Mature, late developing, late maturation, late ripening, total maturation, gravid, vitellogenic, ripe, partially spent, fully developed, prespawning, running ripe, final OM, spawning, gravid, ovulated	Large ovaries, blood vessels prominent. Individual oocytes visible macroscopically. Vtg3 oocytes present or POFs present in batch spawners. Atresia of vitellogenic and/or hydrated oocytes may be present. Early stages of OM can be present. *Actively spawning subphase*: oocytes undergoing late GVM, GVBD, hydration, or ovulation.
Regressing (cessation of spawning)	Spent, regression, postspawning, recovering	Flaccid ovaries, blood vessels prominent. Atresia (any stage) and POFs present. Some CA and/or vitellogenic (Vtg1, Vtg2) oocytes present.
Regenerating (sexually mature, reproductively inactive)	Resting, regressed, recovering, inactive	Small ovaries, blood vessels reduced but present. Only oogonia and PG oocytes present. Muscle bundles, enlarged blood vessels, thick ovarian wall and/or gamma/delta atresia or old, degenerating POFs may be present.

Table 2. Standardised terminology for the histological classification of male fish gonads as described by Brown-Peterson et al. (2011) in their Table 3 and used by this study.

TABLE 3. Macroscopic and microscopic descriptions of the phases in the reproductive cycle of male fishes. Timing within each phase is species dependent. Some criteria listed for phases may vary depending on species, reproductive strategy, or water temperature. Subphases that apply to all fishes are listed; additional subphases can be defined by individual researchers (GE = germinal epithelium; Sc1 = primary spermatocyte; Sc2 = secondary spermatocyte; Sg1 = primary spermatogonia; Sg2 = secondary spermatogonia; St = spermatid; Sz = spermatozoa).

Phase	Previous terminology	Macroscopic and histological features
Immature (never spawned)	Immature, virgin	Small testes, often clear and threadlike. Only Sg1 present; no lumen in lobules.
Developing (testes beginning to grow and develop)	Maturing, early developing, early maturation, ripening	Small testes but easily identified. Spermatocysts evident along lobules. Sg2, Sc1, Sc2, St, and Sz can be present in spermatocysts. Sz not present in lumen of lobules or in sperm ducts. GE continuous throughout. *Early developing subphase*: Sg1, Sg2, and Sc1 only.
Spawning Capable (fish are developmentally and physiologically able to spawn in this cycle)	Late developing, mid-maturation, late maturation, late ripening, ripe, partially spent, running ripe, spawning	Large and firm testes. Sz in lumen of lobules and/or sperm ducts. All stages of spermatogenesis (Sg2, Sc, St, Sz) can be present. Spermatocysts throughout testis, active spermatogenesis. GE can be continuous or discontinuous. *Actively spawning subphase* (macroscopic): milt released with gentle pressure on abdomen. Histological subphases based on structure of GE. *Early GE*: continuous GE in all lobules throughout testes. *Mid-GE*: continuous GE in spermatocysts at testis periphery, discontinuous GE in lobules near ducts. *Late-GE*: discontinuous GE in all lobules throughout testes.
Regressing (cessation of spawning)	Spent, regression, postspawning, recovering	Small and flaccid testes, no milt release with pressure. Residual Sz present in lumen of lobules and in sperm ducts. Widely scattered spermatocysts near periphery containing Sc2, St, Sz. Little to no active spermatogenesis. Spermatogonial proliferation and regeneration of GE common in periphery of testes.
Regenerating (sexually mature, reproductively inactive)	Resting, regressed, recovering, inactive	Small testes, often threadlike. No spermatocysts. Lumen of lobule often nonexistent. Proliferation of spermatogonia throughout testes. GE continuous throughout. Small amount of residual Sz occasionally present in lumen of lobules and in sperm duct.

Data analysis

To determine the size at maturity the reproductive phases were first grouped into two categories, either immature (immature or developing) or mature (all other reproductive phases). These were recorded alongside the fork length (FL) or total length (TL) and their assigned sex. This raw data was grouped into 20 mm length categories and the proportion of mature individuals was calculated.

In order to estimate the length (mm) at 50% (L_{50}) and 95% (*L95*) sexual maturity, a logistic binomial regression was first fitted to the raw maturity data using the generalized linear function (glm) in the software package R (R Core Team 2020). From which L_{50} and *L95* could be estimated using the logistic equation:

$$ x = \frac{log\left(\frac{p}{1-p}\right) - \alpha}{\beta_1} $$

Where χ is either L_{50} or L_{95} and *p* is the proportion mature, ie. 0.5 or 0.95 respectively and α and β are parameters that define the shape and location of the fitted sigmoid curve. These calculations followed the steps outlined in the FishR Vignette and R package FSA (Ogle et al. 2020).

Once the size at maturity for males, females and both sexes combined have been determined, we compared those lengths to the length frequency distribution from the stereo-video surveys the aggregations.

Length frequency distributions

We were able to film spawning aggregations of 18 different reef fish species in Palau for a total of 10,722 individual length measurements. Although only 12 of those had the accompanying size at maturity classifications possible. Sample sizes ranged from 148 – 1819 length measurements depending on the species. For all these species, we sampled on at least two separate days and some species at multiple aggregation sites in Palau. For one species, *Plectropomus areolatus,* these were also filmed in Pohnpei, Federated States of Micronesia (65000 km from Palau) to for comparisons to the size of fish in Palau and existing size at maturity estimates derived from that location.

To display the length frequencies we plotted the lengths as frequency histograms and overlayed a probability density curve using the ggplot2 package in R (R Core Team 2020). A probability density function (geom_density in ggplot) was used as it creates a kernel density estimate based on a continuous distribution of data (rather than frequency histogram which is based on discrete data). This facilitates comparisons of the shape of the distribution of any probability distribution when sample sizes and the shape of the distribution differs. We can then compare the L_{50} value on the x-axis to the y-intercept on the probability density curve. When

averaged across all aggregating species, a probability density value can provide a value used to predict L_{50} from only length frequency distributions if there is low variation between the species.

We also produced cumulative relative frequency (CRF) plots based on the left-hand side of the length frequency distribution. This is commonly modelled with an assumed logistic shape, but to avoid making any assumption about form we plotted this cumulative distribution using stat_ecdf (empirical cumulative distribution function) in ggplot. To only focus on the left-hand side of the curve, the peak density values were first determined then the data was trimmed to only use lengths below this peak value. The cumulative frequency distribution is used to calculate length-based selectivity (*SL*) percentages. For example, there is growing evidence that SL_{50}% of fishery catches, coincides around the size of maturity as animals emerge from their juvenile habitat when they become sexually mature and become susceptible to capture. We therefore had an *a priori* expectation that the coincidence of the size at maturity values would be in the rage of the 25th - 50th percentiles of the cumulative distribution.

Comparison to fishery catch data

Length data from fishery catches was compiled from multiple sources in Palau between the years 2013-2017. This included the database from length measuring projects as part of Palau's northern reefs fisheries management project (Prince et al. 2015b), the creel and market survey by SPC in 2014 (Moore et al. 2015), PICRC northern reefs fishery-dependent data collection in 2015-2016, The 2015 fishery creel and market survey in Palau (Lindfield 2016), reef fish measurements collected during the 2015 and 2016 PSFA Etpison Cup (Lindfield, unpublished data) and the year-long market sampling by the University of Guam and PICRC (Cuetos-Bueno, unpublished data).

Results and discussion

Summaries for all species sampled

In total 1325 fish from twelve species were dissected to estimate size at maturity values. The size at maturity L_{50} and L_{95} values for each of these species are presented in Table 3.

Table 3: Summary of the size at maturity (L_{50} and L_{95}) for all species sampled. Size at maturity was also estimated using Brown-Peterson at al. (2011)'s 'standardised' criteria and the difference in mm between these values are calculated

Taxa	Gender	n	Size at maturity (mm)		Size at maturity (standardised) (mm)		Smallest mature fish (mm)	Difference between L_{50} (standardised) and L_{50}
			L_{50}	L_{95}	L_{50}	L_{95}		
Caranx melampygus	Combined	137	286	353	259	319	267	-27
	Female	53	305	359	300	314	293	-5
	Male	82	273	335	251	253	267	-22
Ctenochaetus striatus	Combined	69	109	138	102	123	88	-7
	Female	40	108	135	107	123	105	-1
	Male	21	106	149	88	91	88	-18
Epinephelus fuscoguttatus	Combined	37	563	569	563	569	610	0
	Female	32	563	569	563	569	640	0
	Male	5					610	
Epinephelus polyphekadion	Combined	131	357	397	357	397	331	0
	Female	94	358	400	358	400	384	0
	Male	37					331	
Hipposcarus longiceps	Combined	120	251	273	237	272	236	-14
	Female	52	250	269	248	268	244	-2
	Male	56	246	268	201	255	236	-45
Lethrinus obsoletus	Combined	119	212	237	210	234	202	-2
	Female	78	222	240	219	237	211	-3
	Male	39					202	
Lethrinus olivaceus	Combined	129	423	483	411	440	356	-12
	Female	99	423	474	412	441	356	-11
	Male	29					399	
Lethrinus xanthochilus	Combined	133	306	350	296	347	288	-10
	Female	79	306	356	292	355	288	-14
	Male	25					325	
Lutjanus bohar	Combined	144	402	475	323	502	336	-79
	Female	71	422	467	409	470	385	-13
	Male	73	384	466			336	*
Naso lituratus	Combined	127	163	215	126	126	156	-37
	Female	103	151	197	126	126	156	-25
	Male	24	210	234			203	*
Plectropomus areolatus	Combined	114	382	449	374	434	343	-8
	Female	86	383	454	373	435	343	-10
	Male	24					415	
Symphorichthys spilurus	Combined	65	338	370	330	366	318	-8
	Female	38	330	353	330	353	318	0
	Male	27	346	372	314	378	350	-32

It was evident that Brown-Peterson at al. (2011)'s standardised criteria, produced lower estimates of L_{50}, especially for male fish. Differences ranged from 0 when there were no fish classified as 'developing', to 79 mm for the combined sex estimate of *Lutjanus bohar,* as all male fish even at smallest size of 183 mm, were categorised as developing (and hence mature) due to the prevalence of primary spermatogonia in the testes. Another other species for which this was particularly problematic for was *Naso lituratus* where no immature male fish were classified and the overall L_{50} was reduced by 37 mm on a fish with a body size range of 158 mm (122-20 mm), the female L_{50} was also reduced by 25 mm due to prevalence of gonads that showed early stage vitellogenic oocytes but no tertiary vitellogenic oocytes.

Using our classification criteria where we regard developing fish as being immature, we compared the L_{50} values to the length frequency distributions from spawning aggregations (Figure 6). This showed a consistent trend where the L_{50} value coincides with the far left-hand side of the main mode of the length frequency distribution around the size of the smallest fish aggregating. Some species had slightly larger L_{50} values for female fish. The L_{95} value was often midway along the left-hand side of the curve.

If we were to use the standardised criteria, then the L_{50} values would often be less than the smallest fish aggregating to spawn. As fishery stock assessments models assume the size at maturity is the size at which fish become functionally adult and begin producing gametes in proportion to adult body weight, we therefore believe categorising developing fish as being immature is more biologically meaningful for our purposes of fishery assessment and management. We therefore present the following species-specific results for size at maturity using immature and developing fish being classified as immature (classed as 0 on the scale of proportion mature) and all other reproductive phases following Brown-Peterson at al. (2011) being mature (classed as 1 on the scale of proportion mature).
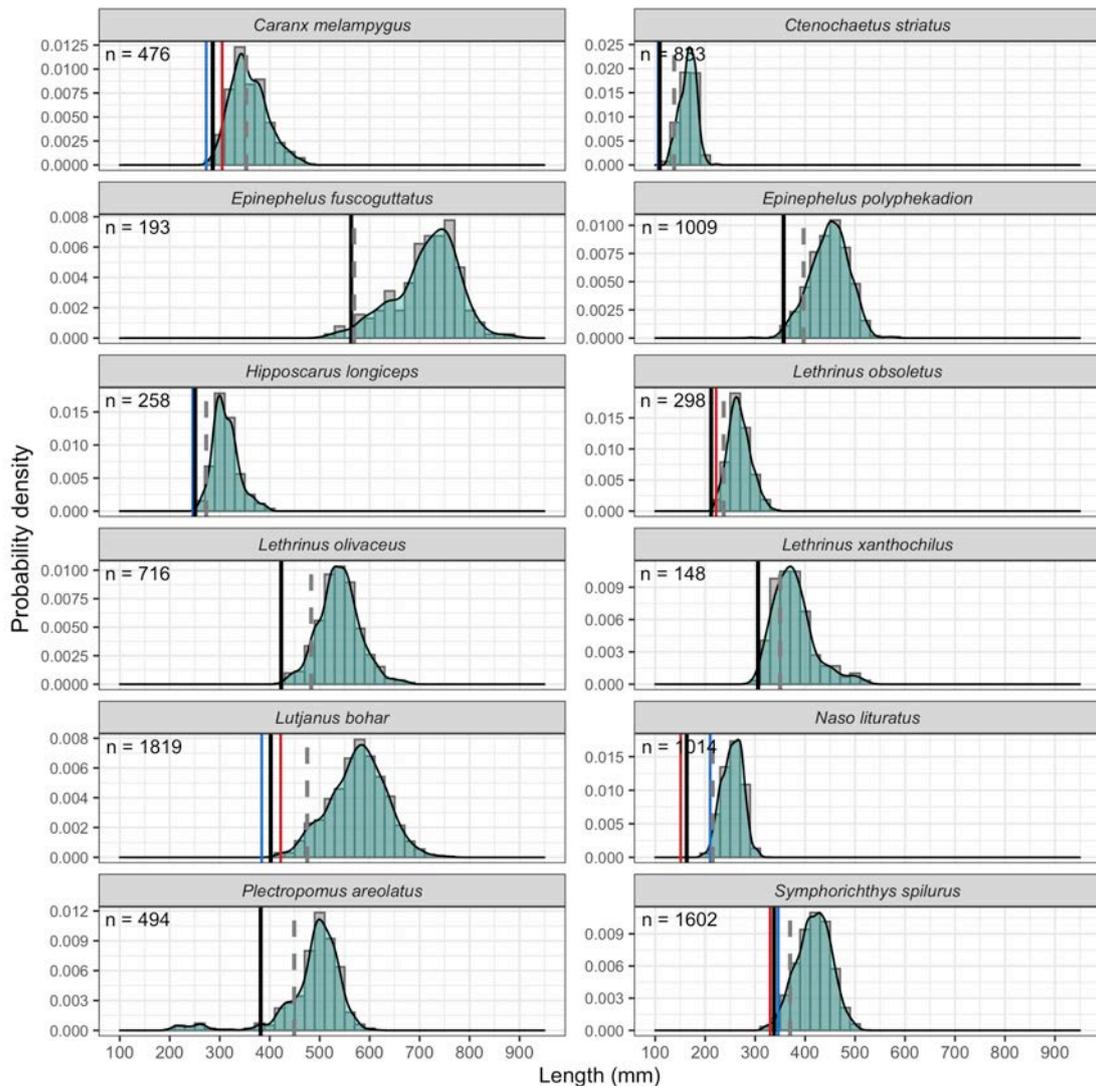
Figure 6. Length frequency distributions for the 12 species sampled with stereo-video at spawning aggregations. Solid vertical lines indicate the size at maturity (L_{50}) values with combined sexes as black, females as red and males as blue lines. The L_{95} combined maturity is plotted as a dashed grey line. Sample size (n) of the number of fish measured is in the top left of each plot.

Caranx melampygus

A total of 137 *C. melampygus* were sampled for maturity and 476 fish measured from spawning aggregations. The estimate of L_{50} for both sexes combined was 286 mm FL (Figure 7), female fish mature slightly larger than males (305 and 273 mm respectively), but a low sample size of immature fish preclude any meaningful comparison between sexes. Two fish of ~ 80 mm were sampled but no gender could be assigned.

Published maturity estimates from other locations are from Caillart et al. (1994) of 260 mm in French Polynesia and by Sudekum et al. (1991) of 375 mm in Hawaii.

Aggregations of *C. melampygus* were filmed at the promontory reef in the southern tip of Peleliu on two separate days, 2 days before and 1 day after the new moon. Comparisons of the length frequencies between days showed that day after the new moon had slightly larger fish, shifting the left-hand side of the length frequency distribution (Figure 8B).

We presume this represents a spawning aggregation but are not certain as there are no confirmed reports of spawning and limited sampling of gonads from the aggregation. We attempted sample collection and of the two fish that we managed to collect from the aggregation without being taken by sharks, both were males with enlarged spawning capable goads. Based on observations by diving guides, these schools only appear around the new moon year-round, and it has been reported by Johannes (1981) and Myers (1999) that 1000 or more fish aggregate at this site to spawn around the new moon.
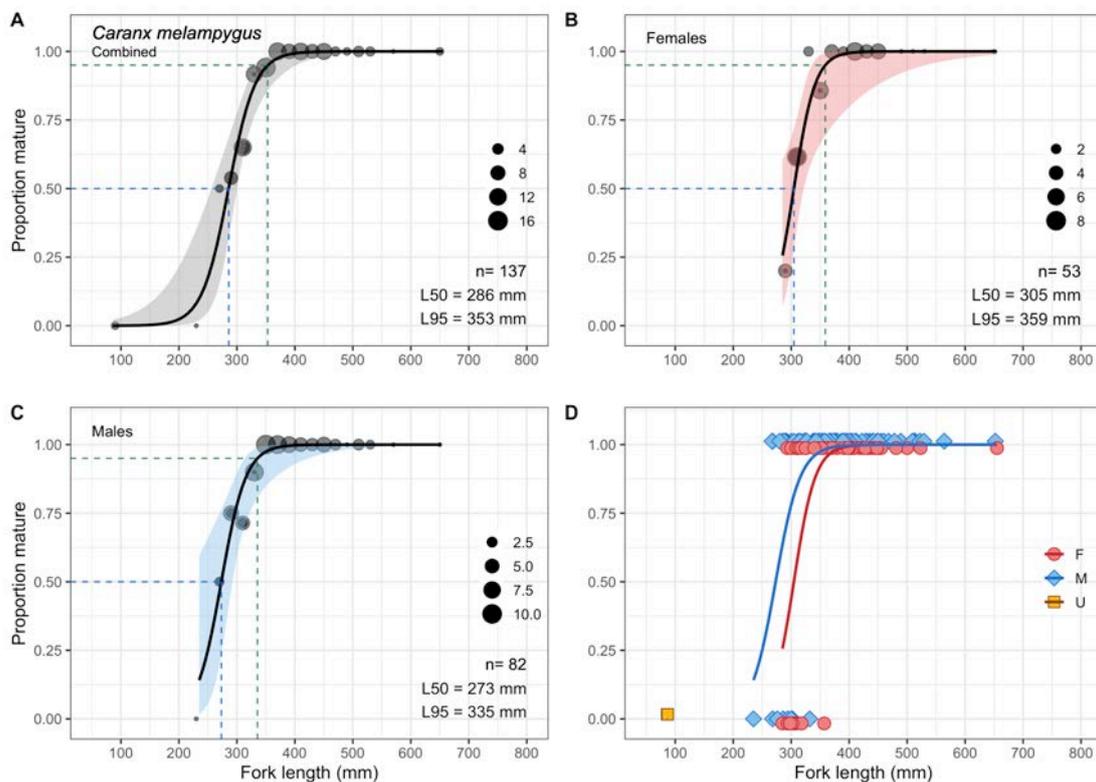
Figure 7. *Caranx melampygus* relationships between length and the proportion mature. (A) Gender combined. (B) Female only. (C) Male only. (D) Genders overlaid showing individual samples; U represents unknown sex. Solid line represents the logistic binomial regression and the shaded area represents the 95% confidence intervals. Samples sizes (n) and estimates of L_{50} and L_{95}, are in bottom right-hand corner of each plot.
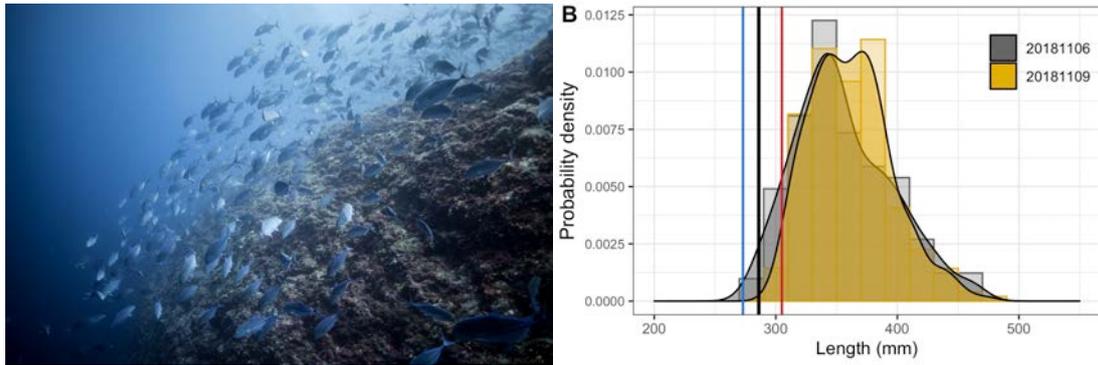
Figure 8. (A) Image of a presumed spawning aggregation of *Caranx melampygus* at Peleliu. (B) Length frequency comparison between the two days when the aggregation was sampled. Solid vertical lines indicate the size at maturity (*L50*) values with combined sexes as black, females as red and males as blue lines
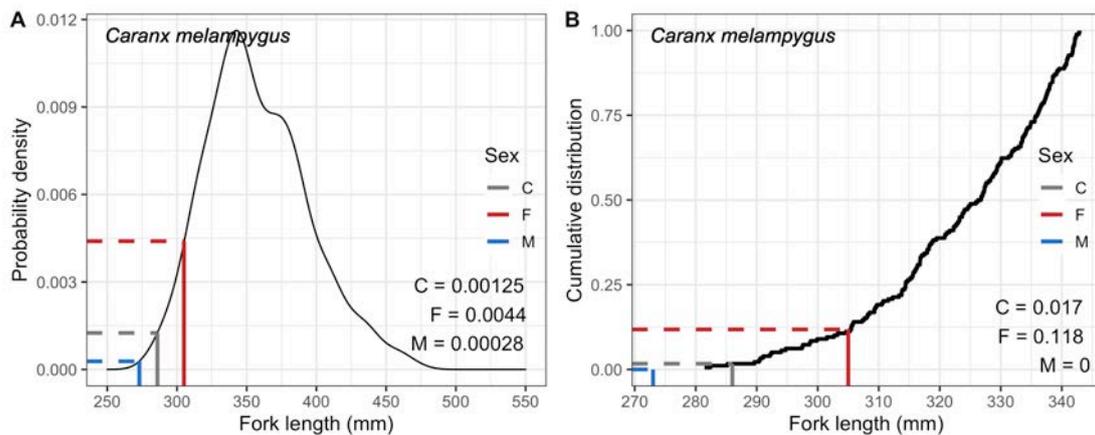
Figure 9. *Caranx melampygus* relationships between the spawning aggregation length frequency distribution and the size of maturity (*L50*) values. (A) Probability density curve and the corresponding y-intercept value that intersects with the maturity values on the x-axis. The probability density value for the gender combined, female and male estimates are displayed in the bottom right of the plot. (B) Cumulative relative frequency plot showing the left-hand side of the length frequency distribution and where the *L50* values correspond to the proportional cumulative distribution.

Ctenochaetus striatus

A total of 69 *C. striatus* were sampled for maturity and 833 fish measured from spawning aggregations. The estimate of *L50* for both sexes combined was 109 mm (Figure 10) and no major differences between sexes despite low samples sizes of immature males. Some small individuals could not be assigned a sex.

There was one other published maturity estimate from American Samoa (150 mm) but was only macroscopically estimated with no *L50* calculated (Ochavillo et al. 2011).

Spawning aggregations were sampled from two locations with two different types of aggregations, first a very large school of several thousand fish were sampled at

Blue Corner, a popular dive site where strong currents are often found. This fish school remained for several days around the new moon in early July 2019 and was sampled 2 days after the new moon when the tidal ranges where maximum for the month. It is unsure if this was actually a spawning aggregation as no fish could be sampled and no spawning witnessed. However, this species was also sampled on the last quarter moon soon after high tide between Big Drop-off and New Drop-off. This time we observed spawning with fish making spawning rushes to release gametes into the warm surface water coming off the reef flat.
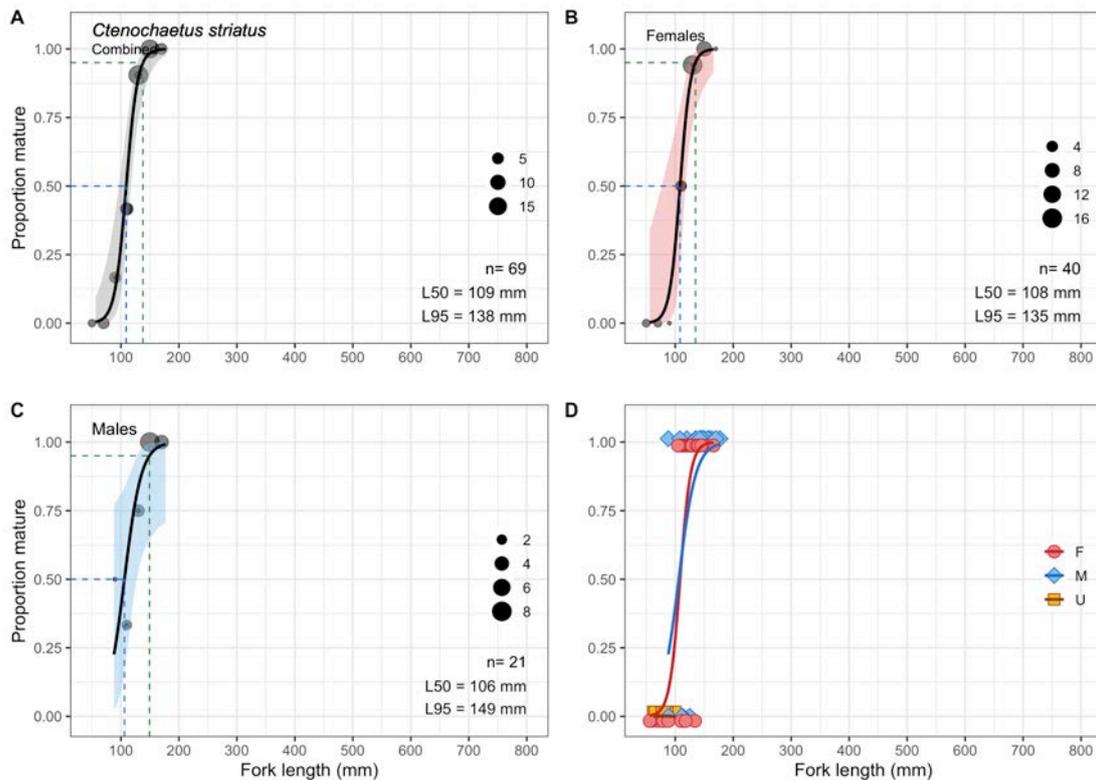
Figure 10. *Ctenochaetus striatus* relationships between length and the proportion mature. (A) Gender combined. (B) Female only. (C) Male only. (D) Genders overlaid showing individual samples; U represents unknown sex. Solid line represents the logistic binomial regression and the shaded area represents the 95% confidence intervals. Samples sizes (n) and estimates of L_{50} and L_{95}, are in bottom right-hand corner of each plot.
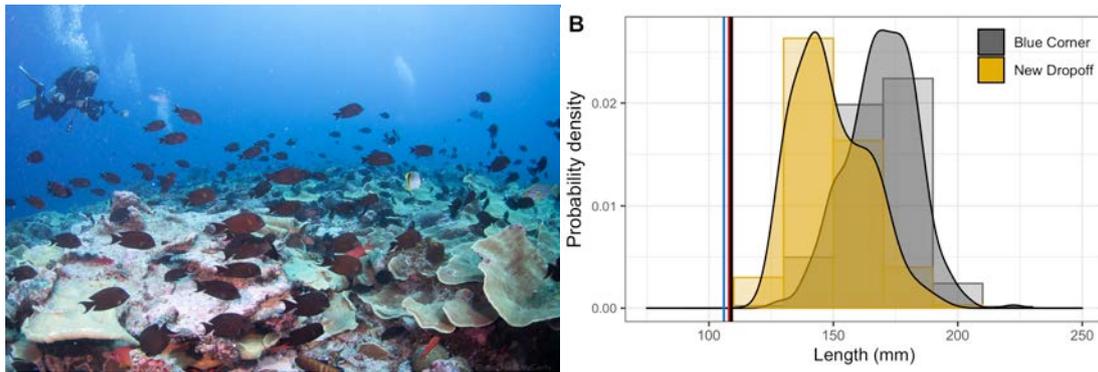
Figure 11. (A) Image of a presumed spawning aggregation of *Ctenochaetus striatus* at Blue Corner. (B) Length frequency comparison between the two sites where aggregations were sampled. Solid vertical lines indicate the size at maturity (L_{50}) values with combined sexes as black, females as red and males as blue lines
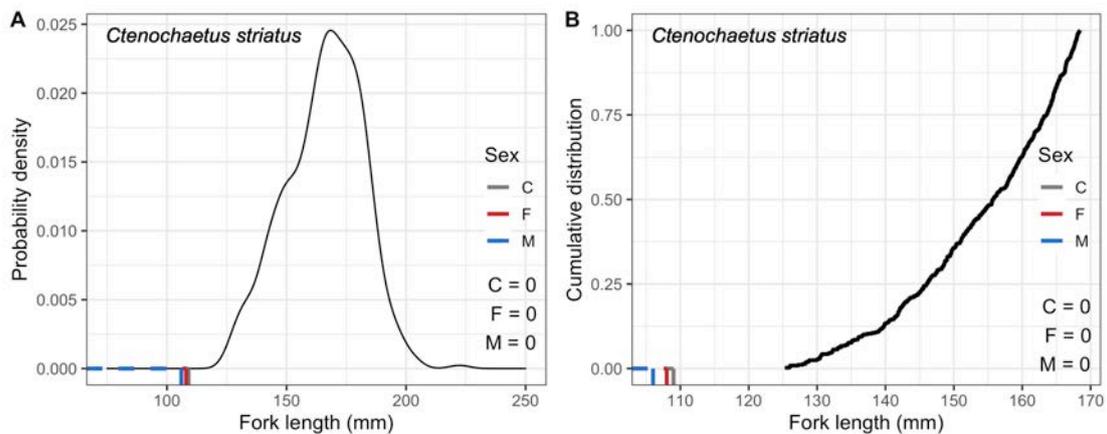
Figure 12. *Ctenochaetus striatus* relationships between the spawning aggregation length frequency distribution and the size of maturity (L_{50}) values. (A) Probability density curve and the corresponding y-intercept value that intersects with the maturity values on the x-axis. The probability density value for the gender combined, female and male estimates are displayed in the bottom right of the plot. (B) Cumulative relative frequency plot showing the left-hand side of the length frequency distribution and where the L_{50} values correspond to the proportional cumulative distribution.

Epinephelus fuscoguttatus

Only 37 *E. fuscoguttatus* were sampled for maturity and 193 fish measured from spawning aggregations. The estimate of L_{50} for both sexes combined was 563 mm TL (Figure 13) which was the same as the female estimate since there were no immature males sampled. With very few samples around the size at maturity, we couldn't confidently estimate a L_{50} but it is likely somewhere between the largest immature fish (515 mm) and the smallest mature fish (610 mm).

Size of maturity estimates have been previously derived for this species on the Great Barrier Reef (GBR) in Australia by Pears et al. (2006). As there was difficulty

determining whether fish were immature or mature and inactive, two different methods were used to calculate the L_{50}. The first using samples of all fish across the year and assessing the percent of all ovaries with signs of current or past spawning activity, this produced an estimate of 408 mm TL. The second method used the percentage of mature active females during the spawning months (called 'effective maturity') and produced a larger estimate of 566 mm, very close to our poorly estimated value.

It is assumed that this species is a protogynous hermaphrodite, changing sex to male from mature females. As the five mature males sampled had atretic oocytes and what resembles a well-developed ovarian lumen. However, with low sample sizes we could not produce solid evidence sex change.

This is a large species with our sampled size range extending from 235 mm to 788 mm. These fish are infrequently landed by fishers in Palau as there is a 7 month ban on grouper retention during their spawning season from the 1st of April to the 31st October each year.

Aggregations were surveyed at 3 different sites with a few fish measured on each of 14 survey days, the two main sites being Ebiil and Ulong Channel, with another 12 fish measured from an aggregation site at Shark City. We compared the lengths between the two main aggregation sites which showed a greater proportion of smaller fish at the Ebiil site compared to Ulong Channel, but with similar minimum and maximum lengths (Figure 14). Spawning has been witnessed at Ulong Channel in the late evening (10 pm) on a new moon at the end of the run-out tide (Niall McCarty pers. comm.).
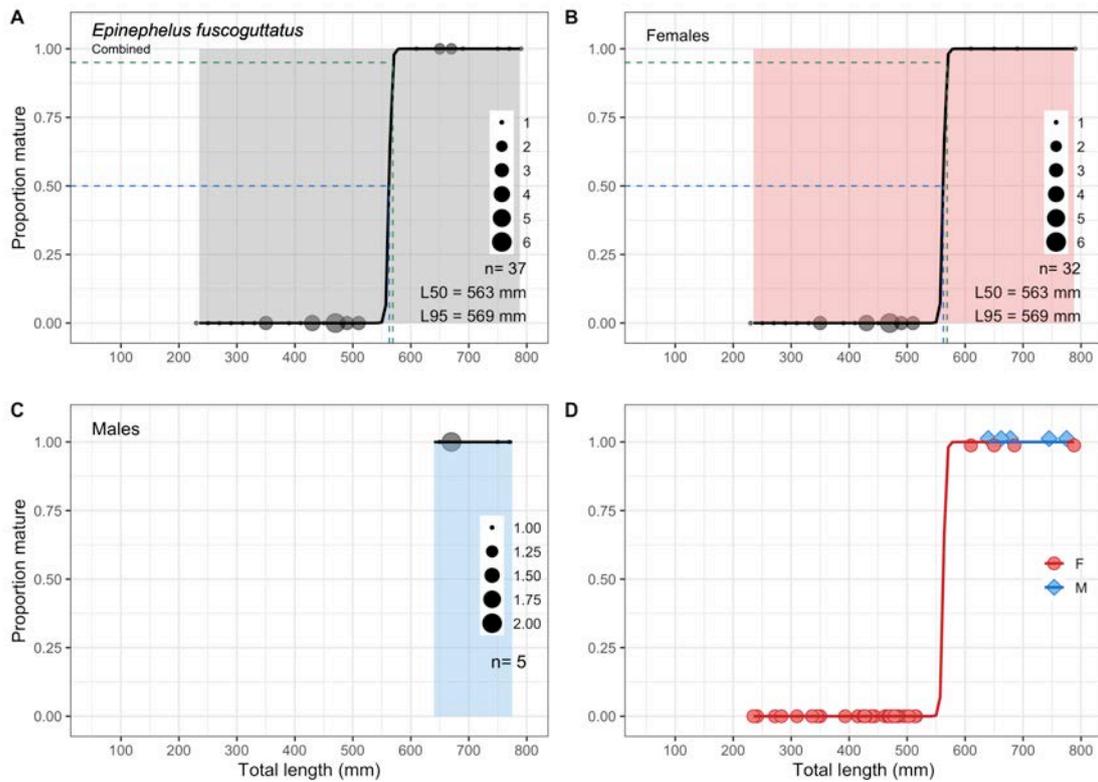
Figure 13. *Epinephelus fuscoguttatus* relationships between length and the proportion mature. (A) Gender combined. (B) Female only. (C) Male only. (D) Genders overlaid showing individual samples. Solid line represents the logistic binomial regression and the shaded area represents the 95% confidence intervals. Samples sizes (n) and estimates of L_{50} and L_{95}, are in bottom right-hand corner of each plot.
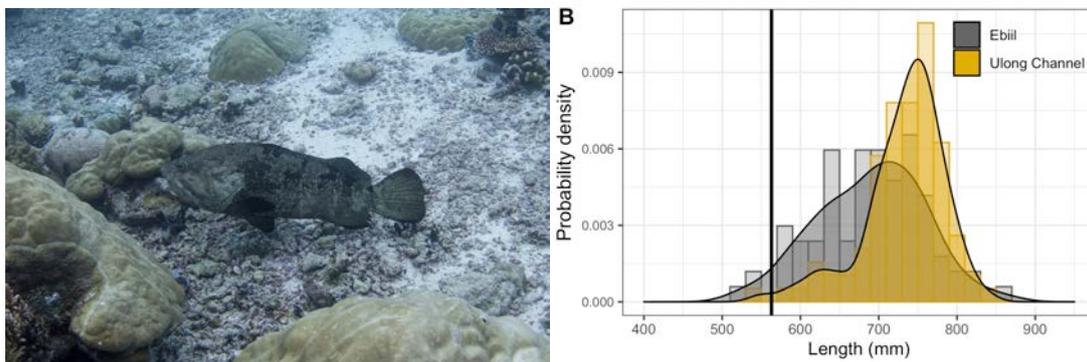
Figure 14. (A) Image of *Epinephelus fuscoguttatus* at the spawning aggregation in Ulong Channel. (B) Length frequency comparison between two aggregation sites where most of the length measurements were taken. The solid vertical line indicates the size at maturity (L_{50}).
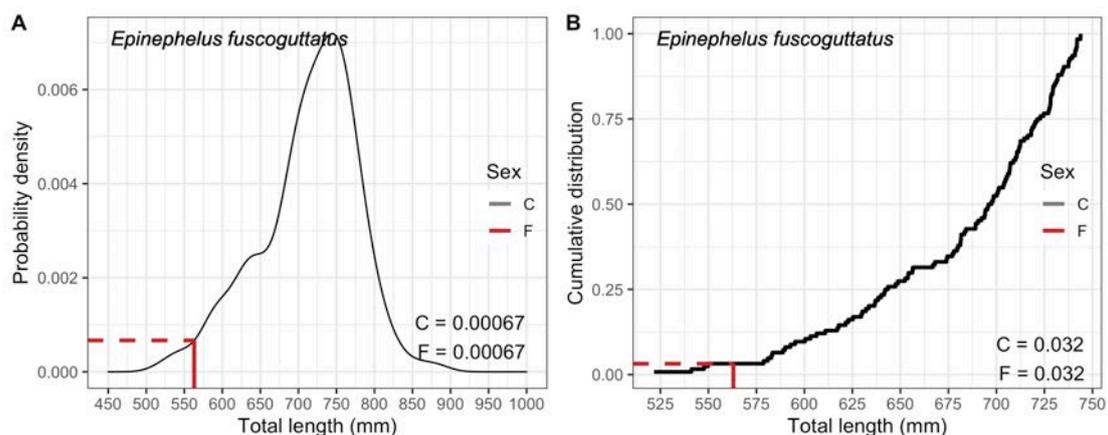
Figure 15. *Epinephelus fuscoguttatus* relationships between the spawning aggregation length frequency distribution and the size of maturity (L_{50}) values. (A) Probability density curve and the corresponding y-intercept value that intersects with the maturity values on the x-axis. The probability density value for the gender combined and female estimates are displayed in the bottom right of the plot. (B) Cumulative relative frequency plot showing the left-hand side of the length frequency distribution and where the L_{50} values correspond to the proportional cumulative distribution.

Epinephelus polyphekadion

A total of 131 *E. polyphekadion* were sampled for maturity and 1009 fish measured from spawning aggregations. The estimate of L_{50} for both sexes combined was 357 mm TL (Figure 16) which was much the same as the female estimate since there were no immature males sampled.

Size of maturity estimates have been previously derived for this species in French Polynesia by Caillart et al. (1994) of 310 mm, by Loubens (1980) of 340mm in New Caledonia, by Maplestone et al. (2009) of 350 mm on the GBR off Australia, by Rhodes et al. (2011) of 327 mm in Pohnpei, and by Rhodes et al. (2020) of 277 mm in Chuuk.

Epinephelus polyphekadion aggregations were filmed on 14 different days at 4 aggregation sites; Ebiil Channel, Ngeruangel, Shark City and Ulong Channel. The two sites with over 450 measurements each - Ebiil Channel and Ulong Channel were compared for length frequencies and found to have similar length distributions (Figure 17B). There was one individual fish measuring 290 mm at Ebiil, and we suspect this fish was immature and not at the site to participate in spawning. Most of the footage was collected from pre-spawning aggregations where the groupers aggregate for several days before the new moon from May – August each year. But footage was also collected from actively spawning fishes at Ulong Channel at night (10-11pm) on the 24th May 2017.
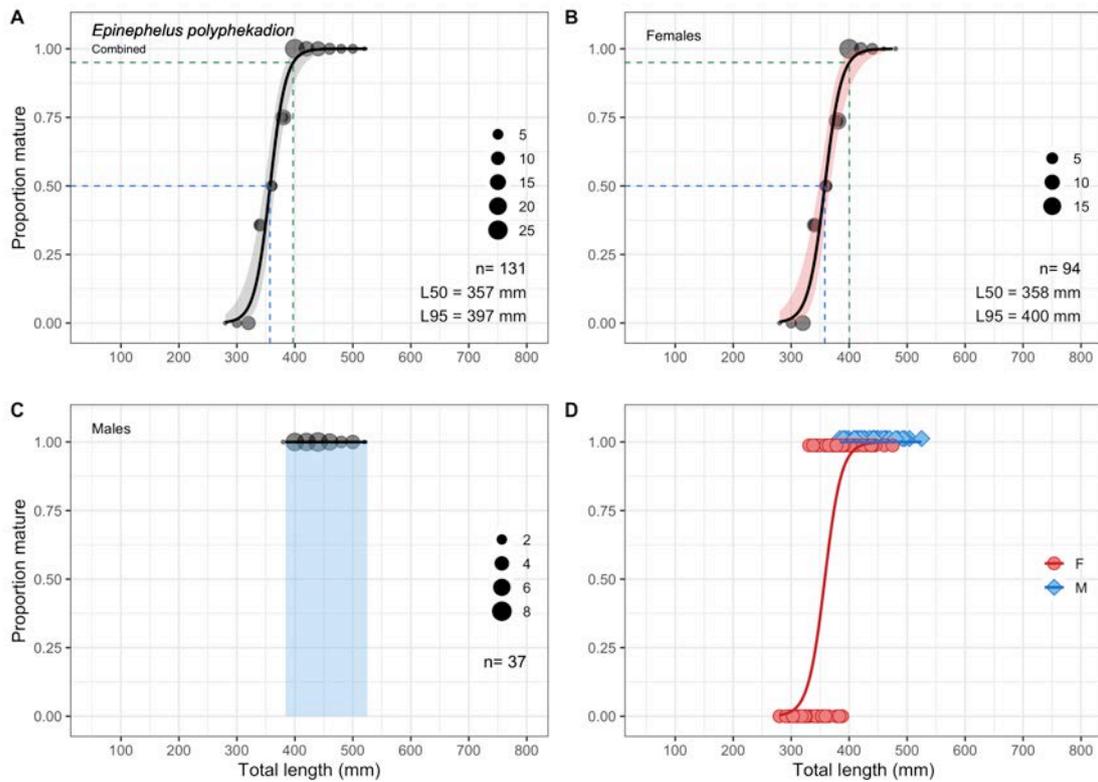
Figure 16. *Epinephelus polyphekadion* relationships between length and the proportion mature. (A) Gender combined. (B) Female only. (C) Male only. (D) Genders overlaid showing individual samples. Solid line represents the logistic binomial regression and the shaded area represents the 95% confidence intervals. Samples sizes (n) and estimates of L_{50} and L_{95}, are in bottom right-hand corner of each plot.
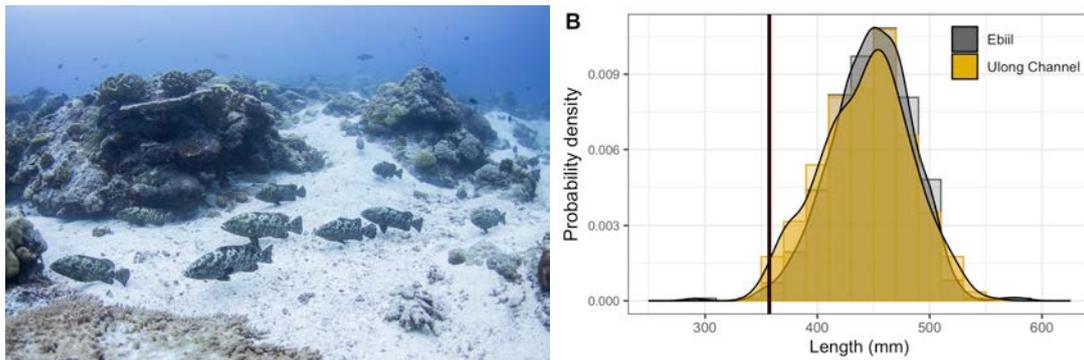
Figure 17. (A) Image of *Epinephelus polyphekadion* at the spawning aggregation in Ulong Channel. (B) Length frequency comparison between two aggregation sites where most of the length measurements were taken. Solid vertical lines indicate the size at maturity (L_{50}) values with combined sexes as black and females as red.
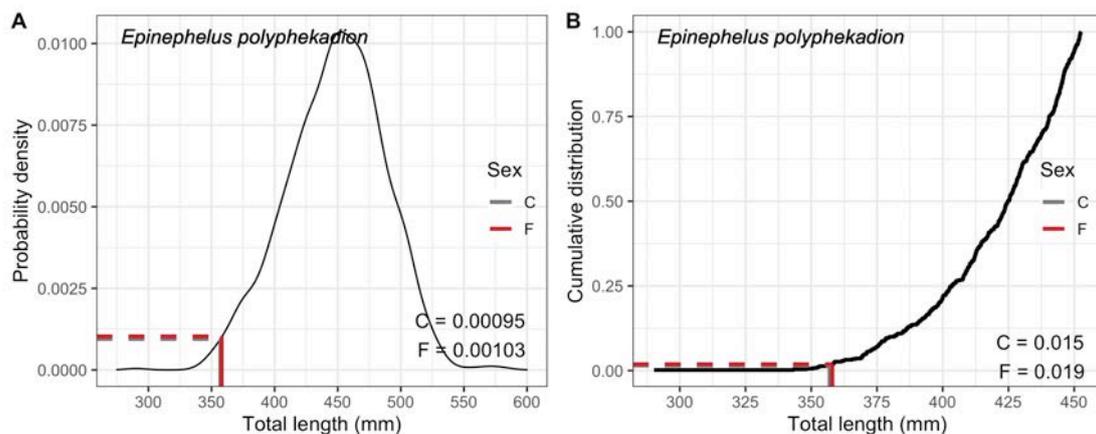
Figure 18. *Epinephelus polyphekadion* relationships between the spawning aggregation length frequency distribution and the size of maturity (L_{50}) values. (A) Probability density curve and the corresponding y-intercept value that intersects with the maturity values on the x-axis. The probability density value for the gender combined and female estimates are displayed in the bottom right of the plot. (B) Cumulative relative frequency plot showing the left-hand side of the length frequency distribution and where the L_{50} values correspond to the proportional cumulative distribution.

Hipposcarus longiceps

A total of 120 *H. longiceps* were sampled for maturity and 258 fish measured from spawning aggregations. The estimate of L_{50} for both sexes combined was 251 mm FL (Figure 19) which was much the same as the female estimate, whereas males matured slightly smaller (246 mm).

Size of maturity estimates have been previously derived for this species in Pohnpei by Taylor and Choat (2014) of 317 mm and in Guam by Taylor and Cruz (2017) of 329 mm. Our estimate is significantly smaller than these estimates.

This species spawns regularly in the hour after high tide at many sites in Palau where the current can sweep the gametes away from the reef. Aggregation size is relatively small, around 20 – 100 fish, although larger aggregations of hundreds or thousands of fish have been infrequently reported in Palau but none of which were sampled. We recorded spawning at four different sites; Bilis, Blue Corner, Shark City, Ulong Sandbar on 7 different days. We compared length frequencies between three of the main sites, Blue Corner, Shark City and Ulong Sandbar to find larger fish at Blue corner and smaller fish at Ulong Sandbar (Figure 20B).
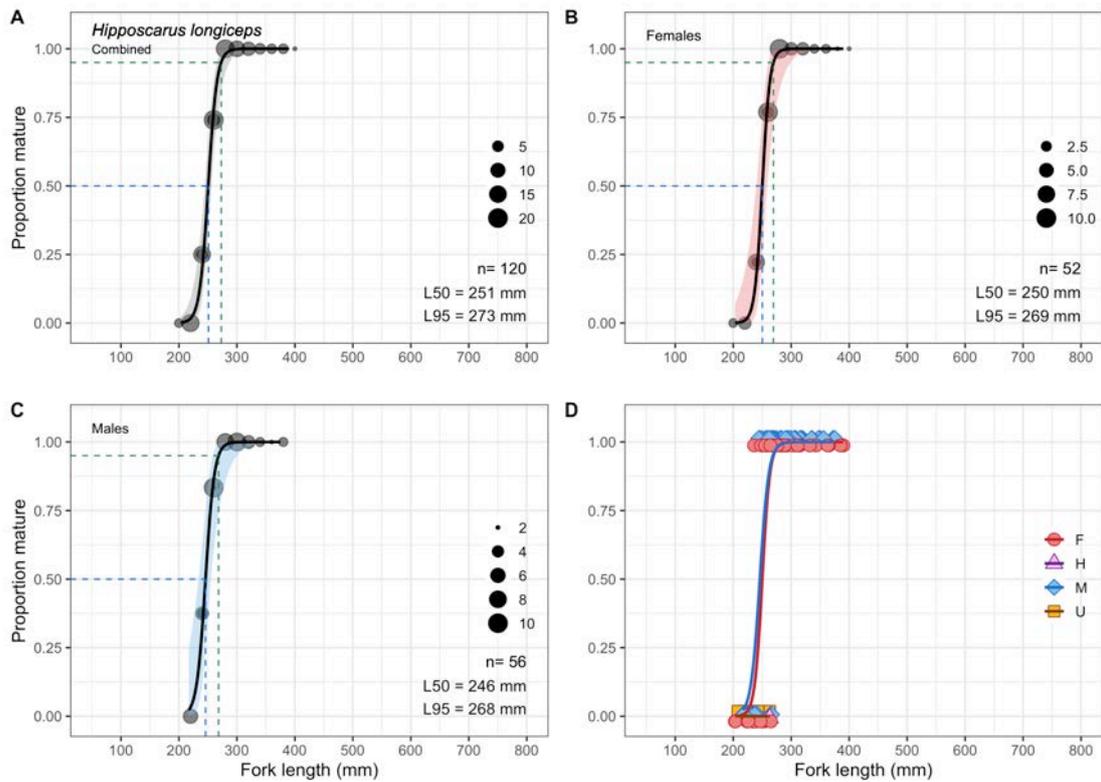
Figure 19. *Hipposcarus longiceps* relationships between length and the proportion mature. (A) Gender combined. (B) Female only. (C) Male only. (D) Genders overlaid showing individual samples where H = hermaphrodites and U = unknown sex. Solid line represents the logistic binomial regression and the shaded area represents the 95% confidence intervals. Samples sizes (n) and estimates of L_{50} and L_{95}, are in bottom right-hand corner of each plot.
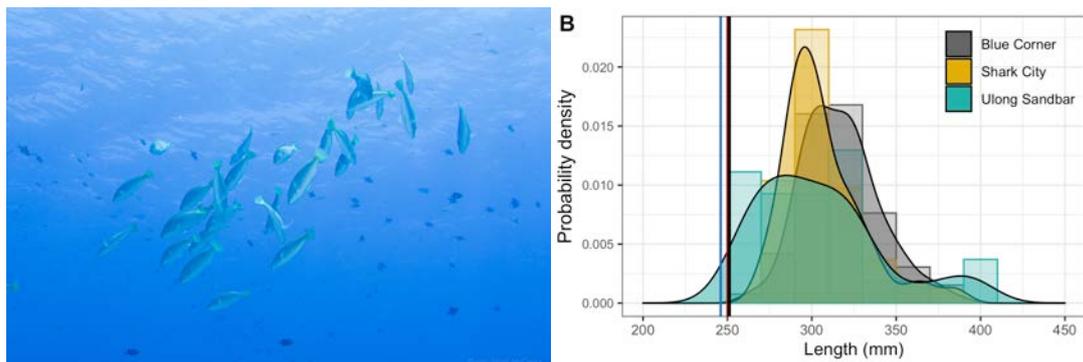
Figure 20. (A) Image of *Hipposcarus longiceps* in the descent from spawning rush at Blue Corner. (B) Length frequency comparison between the three aggregation sites where most of the length measurements were taken. Solid vertical lines indicate the size at maturity (L_{50}) values with combined sexes as black, females as red and males as blue lines
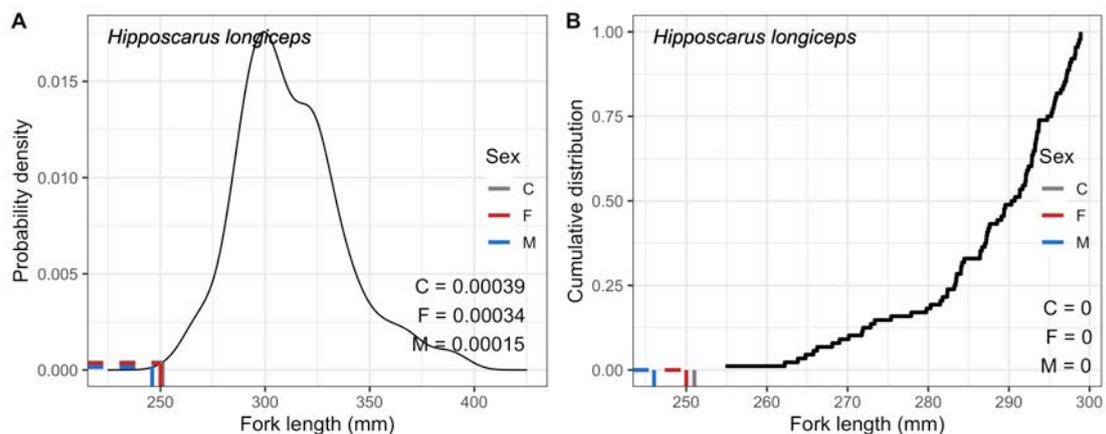
Figure 21. *Hipposcarus longiceps* relationships between the spawning aggregation length frequency distribution and the size of maturity (L_{50}) values. (A) Probability density curve and the corresponding y-intercept value that intersects with the maturity values on the x-axis. The probability density value for the gender combined, female and male estimates displayed in the bottom right of the plot. (B) Cumulative relative frequency plot showing the left-hand side of the length frequency distribution and where the L_{50} values correspond to the proportional cumulative distribution.

Lethrinus obsoletus

A total of 119 *L. obsoletus* were sampled for maturity and 298 fish measured from spawning aggregations. The estimate of L_{50} for both sexes combined was 212 mm FL with the female estimate slightly larger at 222 mm (Figure 22) and no immature males were sampled. We did find two immature hermaphroditic gonads with ovarian and testicular tissue together.

Size of maturity estimates have been previously derived for this species in the Commonwealth of the Northern Mariana Islands by Taylor et al. (2017) of 229 mm FL for females and 199 mm for males. In Guam the L_{50} for was estimated as 210 mm by Taylor (2010). Our samples fall within this range.

Only one spawning aggregation site was sampled, Ulong Sandbar, which is a site where other large spawning aggregations occur, such as the bumphead parrotfish. Numbers of fish are estimated to peak at several thousand fish and they predictably aggregate towards the first quarter moon year-round with numbers building for several days before dissipating from the site on or just after the day of the quarter moon. To see how the length frequency changes between dates and aggregation size, we plotted the October 15th, 2018 date which was 2 days before the first quarter moon when aggregation size was estimated to be ~200 fish and 45 fish were measured. This was compared to March 13th, 2019 one day before the first quarter moon when the aggregation size was estimated at 2000 + fish, of which 253 were measured. Both samples had very similar left-hand sides of the density curves, although the date with the larger sample size also had a greater proportion of larger fish (Figure 23B).
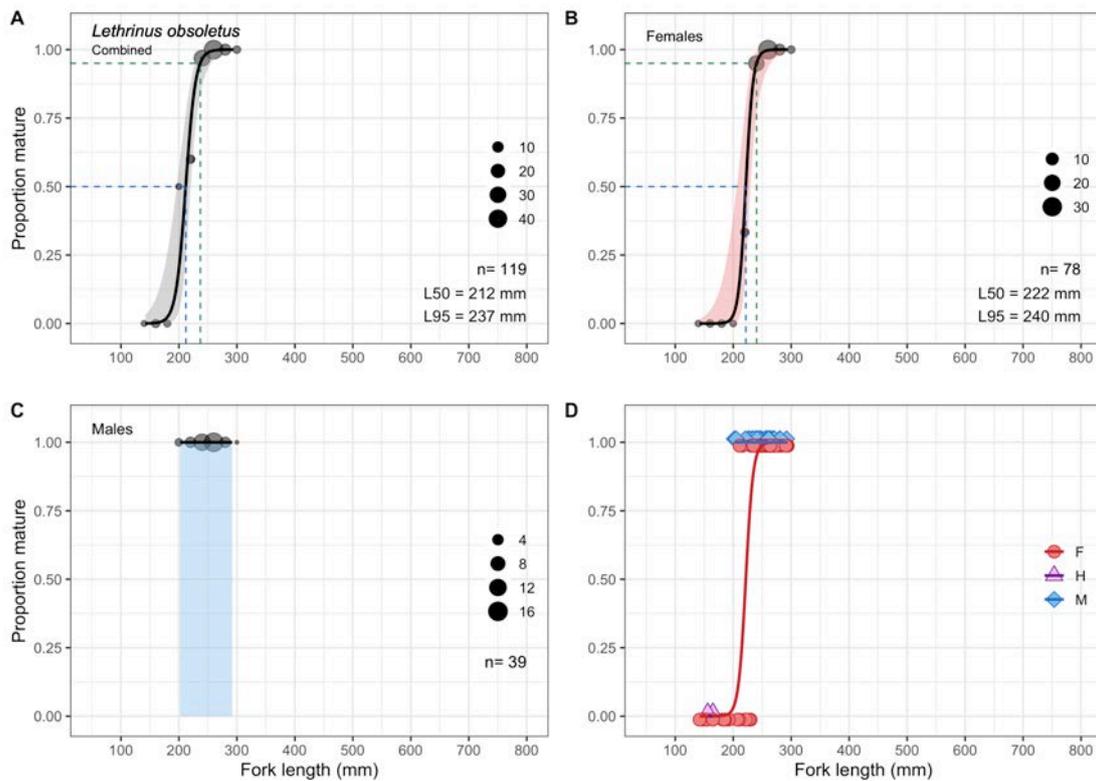
Figure 22. *Lethrinus obsoletus* relationships between length and the proportion mature. (A) Gender combined. (B) Female only. (C) Male only. (D) Genders overlaid showing individual samples where H = hermaphrodites. Solid line represents the logistic binomial regression and the shaded area represents the 95% confidence intervals. Samples sizes (n) and estimates of L_{50} and L_{95}, are in bottom right-hand corner of each plot.
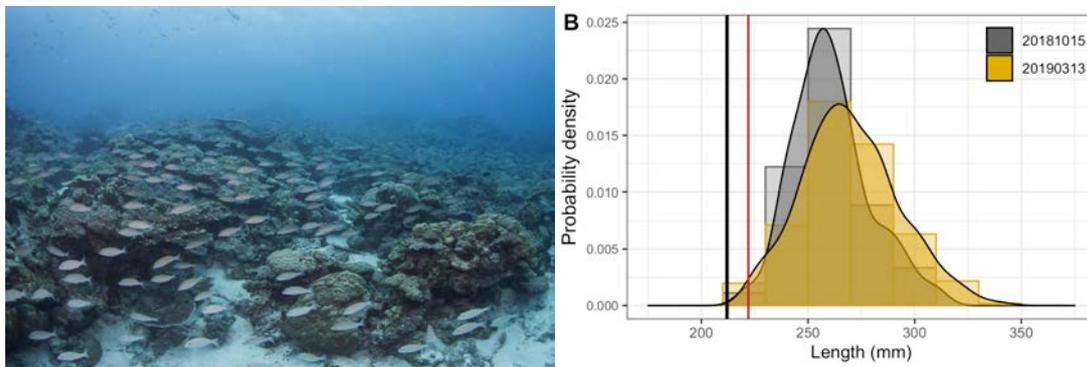
Figure 23. (A) Image of *Lethrinus obsoletus* at the spawning aggregation at Ulong Sandbar. (B) Length frequency comparison between two sample dates. Solid vertical lines indicate the size at maturity (L_{50}) values with combined sexes as black and females as red.

31
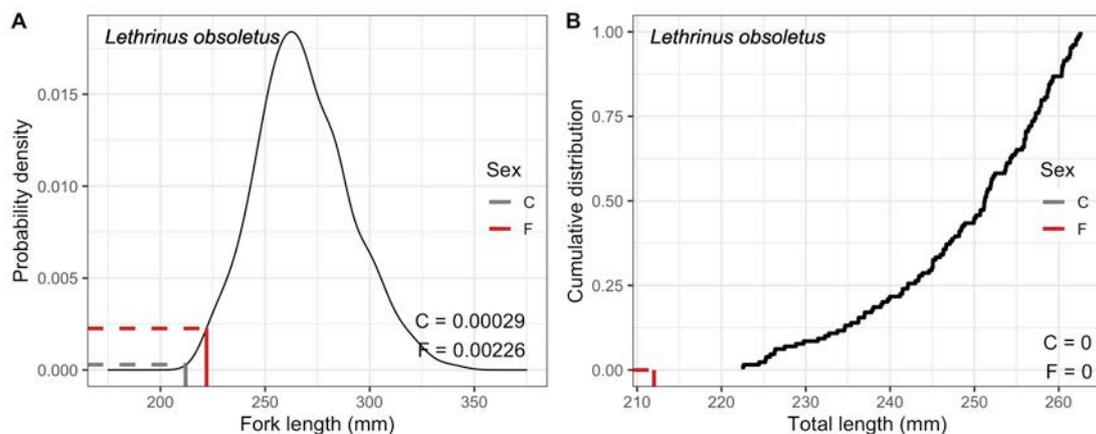
Figure 24. *Lethrinus obsoletus* relationships between the spawning aggregation length frequency distribution and the size of maturity (L_{50}) values. (A) Probability density curve and the corresponding y-intercept value that intersects with the maturity values on the x-axis. The probability density value for the gender combined and female estimates are displayed in the bottom right of the plot. (B) Cumulative relative frequency plot showing the left-hand side of the length frequency distribution and where the L_{50} values correspond to the proportional cumulative distribution.

Lethrinus olivaceus

A total of 129 *L. olivaceus* were sampled for maturity and 716 fish measured from spawning aggregations. The estimate of L_{50} for both sexes combined was 423 mm FL which was the same as the female only data as there were no immature males recorded, and the majority of mature males were larger than the L_{95} value (Figure 25). There are no other published maturity estimates for this species.

Spawning aggregations were sampled at three different sites across 7 days. Shark City was the main site we surveyed this species and we predictably found large numbers (several hundred) of these fish around the new moon, and not at other times. This species is known to form and be caught in aggregations according to Johannes (1981), however we were not able to confirm spawning or sample any fish from the aggregation site (as it is a no-fishing area around a dive site). We deployed time-lapse cameras at this site to capture any early morning or late evening spawning without any confirmation. It is likely they spawn during the night, as with other Lethrinids. Fishermen also report highest catches at night around new moon.

Measurements at the three main aggregation sites (Figure 26B) showed the Ngerael site having larger fish, and this site is located in the far north of Palau where fishing pressure is lower than around the other two sites. The spread of the data at the Bilis site was larger than Shark City, with the latter having the smallest modal peak.
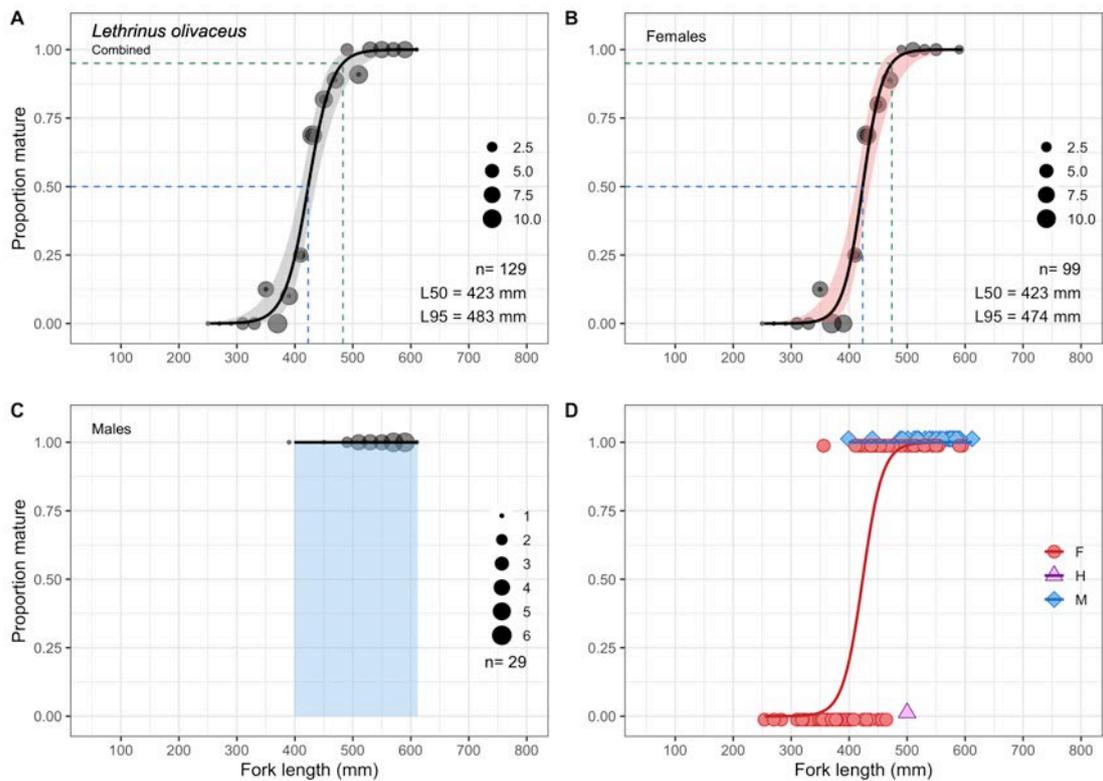
Figure 25. *Lethrinus olivaceus* relationships between length and the proportion mature. (A) Gender combined. (B) Female only. (C) Male only. (D) Genders overlaid showing individual samples where H = hermaphroditic fish. Solid line represents the logistic binomial regression and the shaded area represents the 95% confidence intervals. Samples sizes (n) and estimates of L_{50} and L_{95}, are in bottom right-hand corner of each plot.
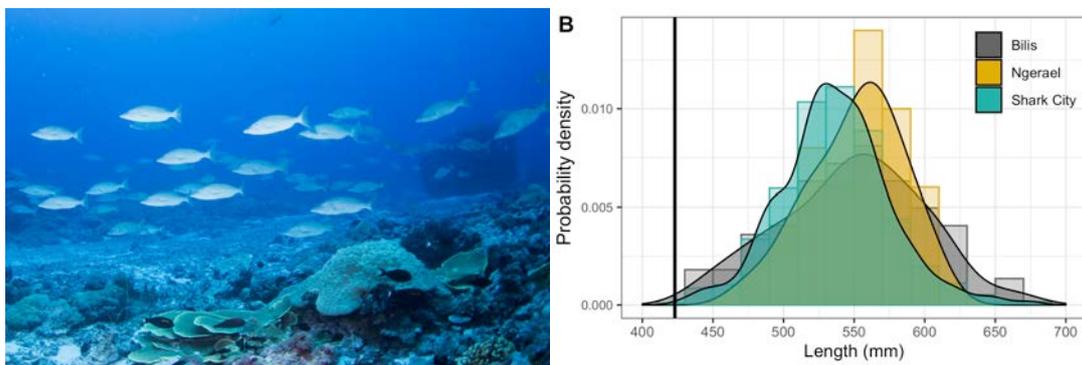
Figure 26. (A) Image of *Lethrinus olivaceus* at the spawning aggregation at Shark City. (B) Length frequency comparison between the three main aggregation sites where length measurements were taken. Solid vertical lines indicate the size at maturity (L_{50}) values with combined sexes as black and females as red.
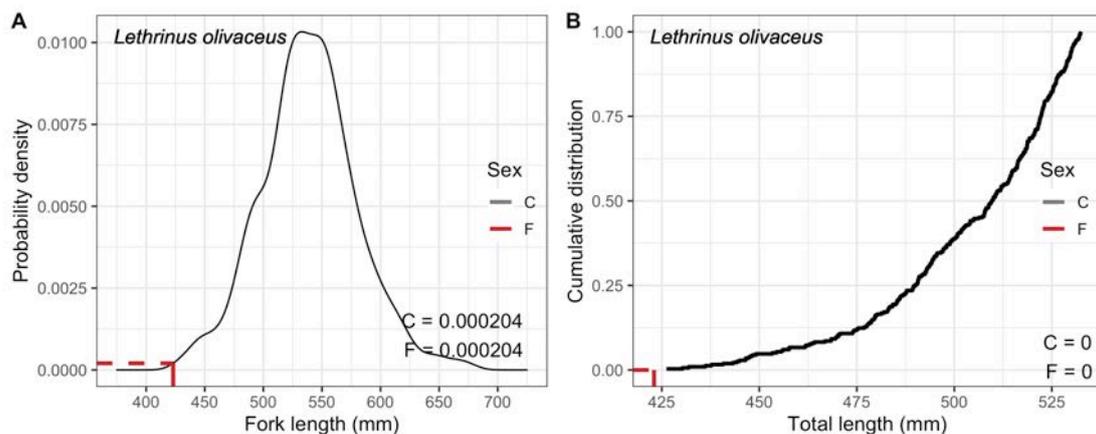
Figure 27. *Lethrinus olivaceus* relationships between the spawning aggregation length frequency distribution and the size of maturity (L_{50}) values. (A) Probability density curve and the corresponding y-intercept value that intersects with the maturity values on the x-axis. The probability density value for the gender combined and female estimates are displayed in the bottom right of the plot. (B) Cumulative relative frequency plot showing the left-hand side of the length frequency distribution and where the L_{50} values correspond to the proportional cumulative distribution.

Lethrinus xanthochilus

A total of 133 *L. xanthochilus* were sampled for maturity but only 148 fish measured from spawning aggregations. The estimate of L_{50} for both sexes combined was 306 mm FL which was the same as the female only data as there were no immature males recorded and the majority of mature males were larger than the L_{50} value (Figure 28).

Size of maturity estimates have been previously derived for this species in American Samoa by Taylor et al. (2018) with an L_{50} of 300 mm FL for females. Their study provided some evidence of both pre- and post-maturational sex change and we also recorded immature hermaphroditic individuals and one that appears to be going through a mature transition from female to male. However, without larger sample sizes and age-based data it is difficult to be certain about the developmental ontogeny of this species in Palau.

Presumed spawning aggregations were primarily sampled at Shark City at times when *L. olivaceus* was aggregating. Again, these fish were only there in elevated numbers during the new moon phase, however numbers were substantially less than *L. olivaceus* and fish were difficult to approach closely for measurements. We are not sure of actual spawning from these aggregations and if so, it likely occurs at night as with other Lethrinids. We also sampled a mere 11 fish at the Bilis site which showed the left-hand side of the density curve pushed to the right compared to data from shark City and would not be a reliable length distribution on its own (Figure 29B). But together, despite a small sample size, as with other species these data align where the L_{50} intersects the tail of the curve around the size of the smallest fish (Figure 30).
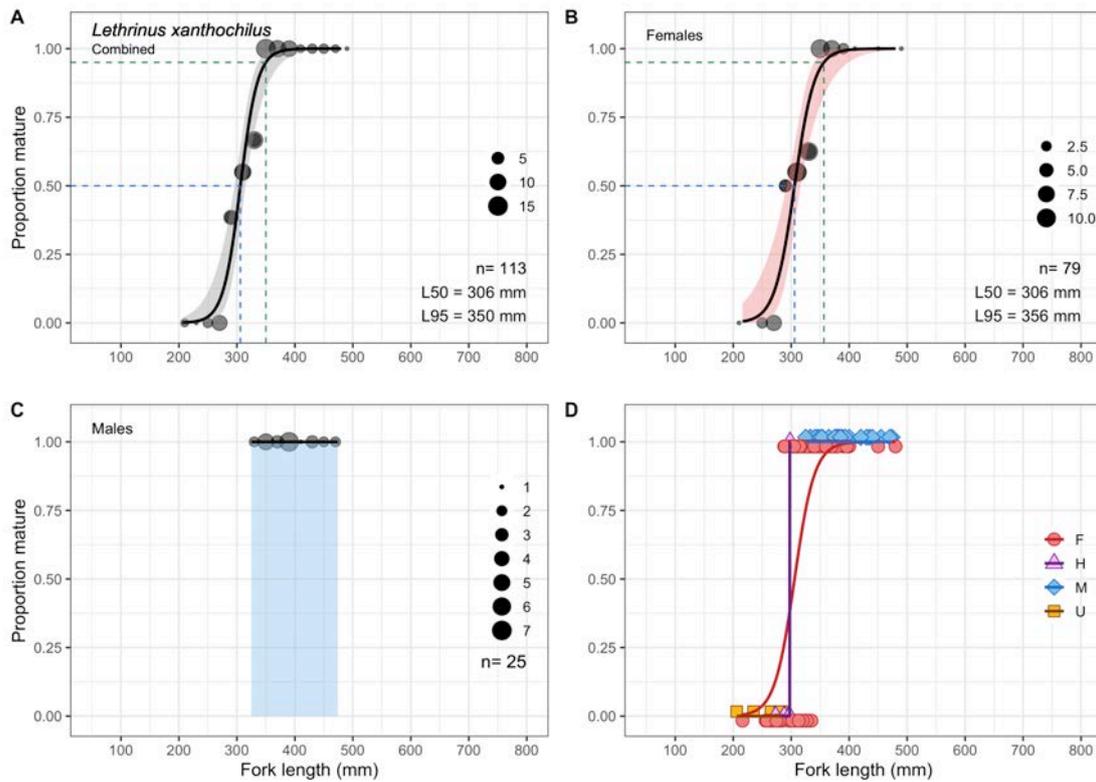
Figure 28. *Lethrinus xanthochilus* relationships between length and the proportion mature. (A) Gender combined. (B) Female only. (C) Male only. (D) Genders overlaid showing individual samples where H = hermaphrodites and U = unknown sex. Solid line represents the logistic binomial regression and the shaded area represents the 95% confidence intervals. Samples sizes (n) and estimates of L_{50} and L_{95}, are in bottom right-hand corner of each plot.
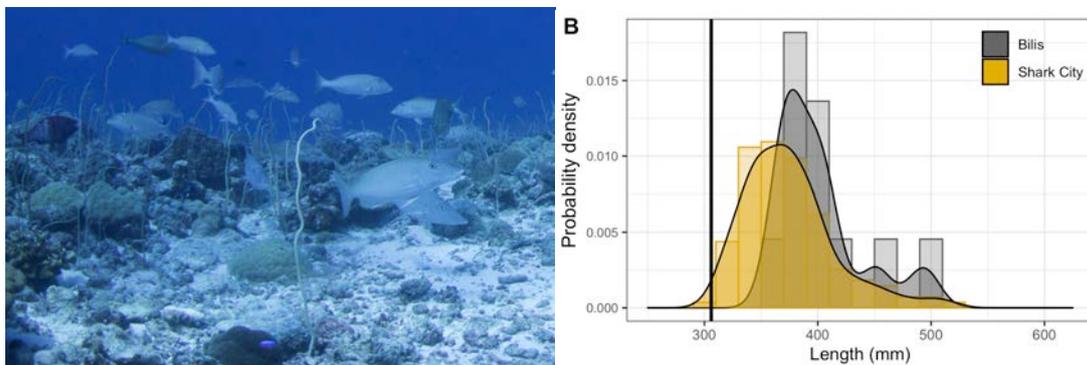
Figure 29. (A) Image of *Lethrinus xanthochilus* at the spawning aggregation at Shark City mixed with *Lethrinus olivaceus*. (B) Length frequency comparison between the two main aggregation sites where length measurements were taken. Solid vertical lines indicate the size at maturity (L_{50}) values with combined sexes as black and females as red.

35
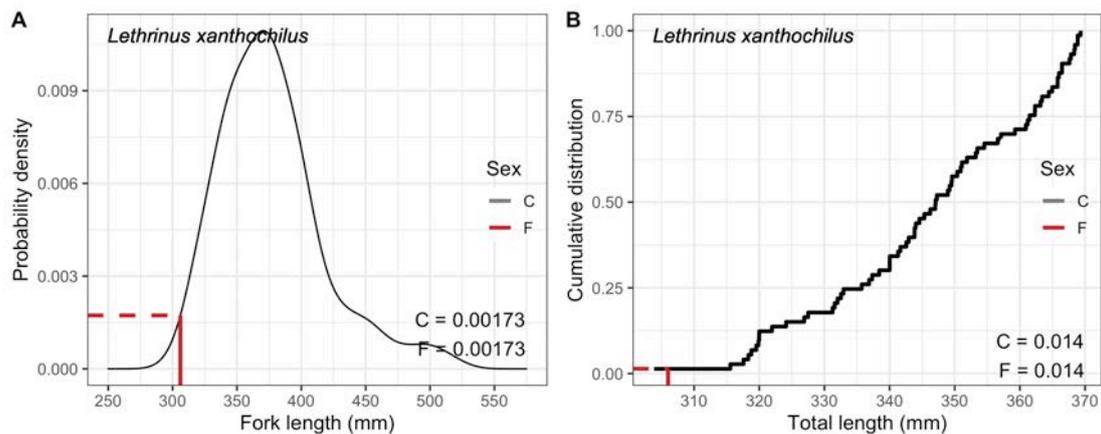
Figure 30. *Lethrinus xanthochilus* relationships between the spawning aggregation length frequency distribution and the size of maturity (*L50*) values. (A) Probability density curve and the corresponding y-intercept value that intersects with the maturity values on the x-axis. The probability density value for the gender combined, female estimates are displayed in the bottom right of the plot. (B) Cumulative relative frequency plot showing the left-hand side of the length frequency distribution and where the *L50* values correspond to the proportional cumulative distribution.

Lutjanus bohar

A total of 144 *L. bohar* were sampled for maturity and 1819 fish measured from spawning aggregations. The estimates of L_{50} for both sexes combined was 402 mm FL and 422 mm for females (Figure 31). Males matured considerably smaller than females at 384 mm.

Previously, maturity estimates have been derived for this species by Longenecker *et al.* (2014) of 430 mm for females and < 300 mm for males off the north coast of PNG, by Wright *et al.* (1986) of 450 mm for females at New Ireland, PNG and by Marriott *et al.* (2010) who estimated 428 mm for females on the GBR off Australia and could not estimate maturity for males due to small number of immature fish but estimated maturity at a size of 200-300 mm based on the smallest mature male at a size of 248 mm FL.

Lutjanus bohar aggregations were only sampled at Shark City and measurements were analysed from 8 different days over 5 years. These fish form large spawning aggregations of 2000-7000 fish in the early mornings for several days before the full moon. They actively spawn during this time and footage was analysed from pre-spawn, actively spawning and post-spawning fish over a period of 1-1.5 hrs on each survey day. We compared length frequencies between years and with the exception of the 2019 survey they were fairly consistent (Figure 32B). The 2019 data was skewed to the larger fish and although the smallest and largest measurements were consistent with previous years it shifted the left-hand side of the probability density curve. We are not sure what this could be, but speculate that these 190 measurements from a single survey day in 2019 may have inadvertently measured a greater proportion of female fish that would likely be larger than mixed female fish,

but nonetheless suggest multiple days of measurements are important for generating reliable length frequency distributions.
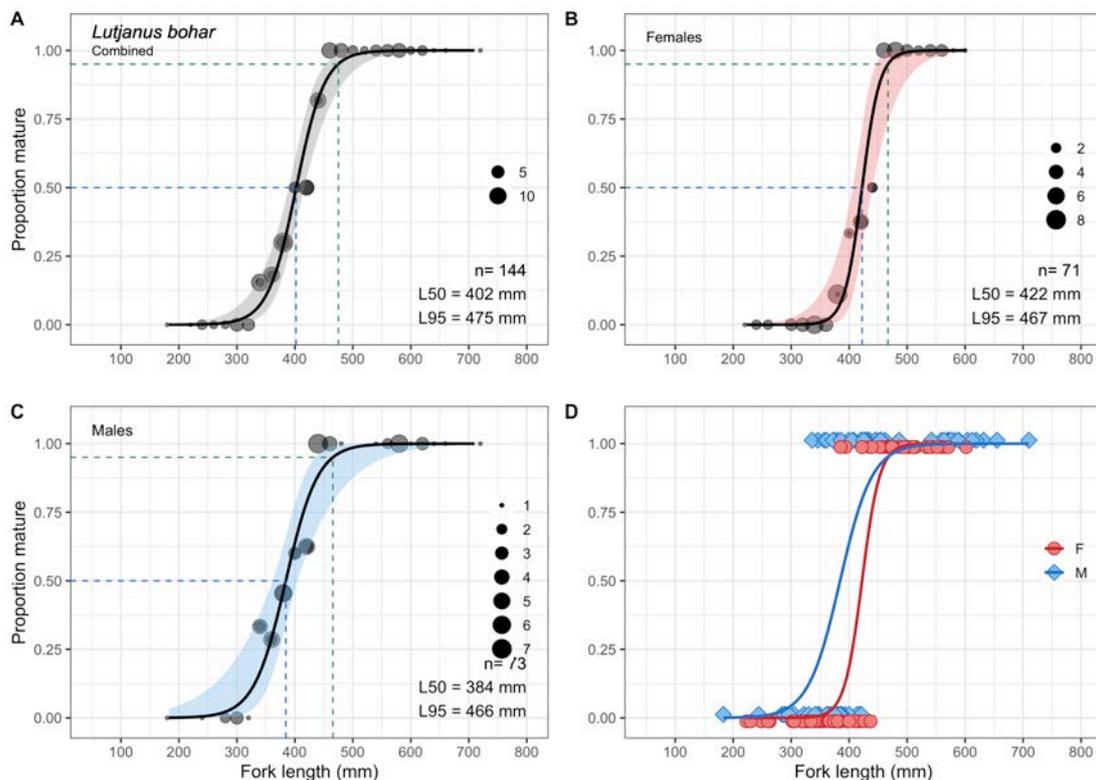
Figure 31. *Lutjanus bohar* relationships between length and the proportion mature. (A) Gender combined. (B) Female only. (C) Male only. (D) Genders overlaid showing individual samples. Solid line represents the logistic binomial regression and the shaded area represents the 95% confidence intervals. Samples sizes (n) and estimates of L_{50} and L_{95}, are in bottom right-hand corner of each plot.
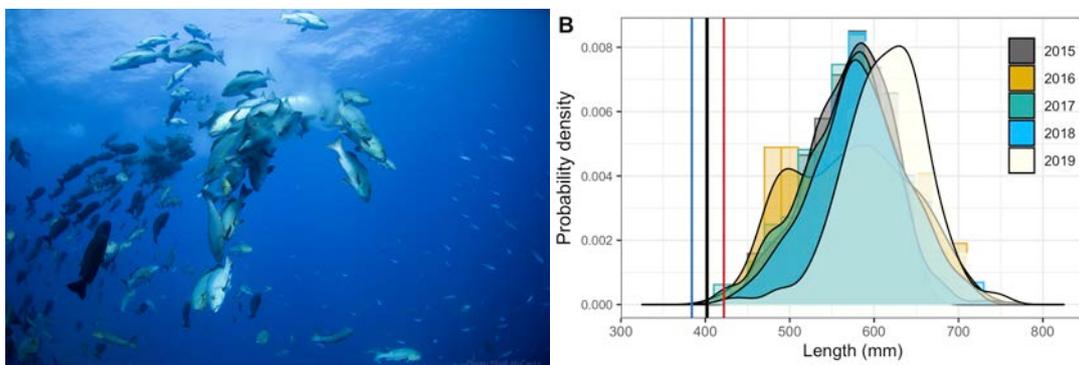
Figure 32. (A) Image of *Lutjanus bohar* at the spawning aggregation at Shark City. (B) Length frequency comparison between 5 years of surveys when length measurements were taken. Solid vertical lines indicate the size at maturity (L_{50}) values with combined sexes as black and females as red.
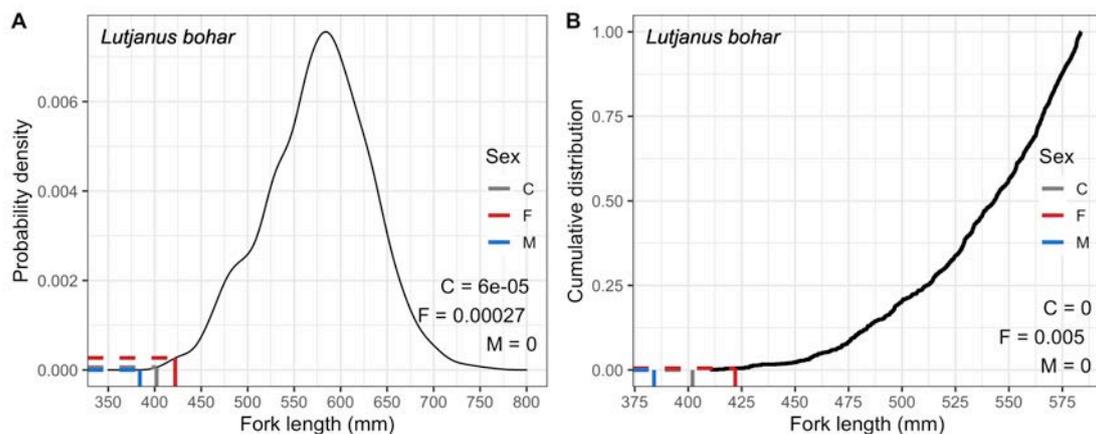
Figure 33. *Lutjanus bohar* relationships between the spawning aggregation length frequency distribution and the size of maturity (*L₅₀*) values. (A) Probability density curve and the corresponding y-intercept value that intersects with the maturity values on the x-axis. The probability density value for the gender combined, female and male estimates are displayed in the bottom right of the plot. (B) Cumulative relative frequency plot showing the left-hand side of the length frequency distribution and where the *L₅₀* values correspond to the proportional cumulative distribution.

Naso lituratus

A total of 127 *N. lituratus* were sampled for maturity and 1014 fish measured from spawning aggregations. The estimates of L_{50} for both sexes combined was 163 mm FL with females maturing at a smaller size (151 mm) and males at larger size (210 mm) (Figure 34). As these fish are sexually dimorphic, samples chosen from the market were biased towards females as they are a more reliable indicator of maturation for the purposes of fishery assessments.

A previous study attempted to estimate the size at maturity in Guam and Pohnpei in Micronesia (Taylor et al. 2014). Using sample sizes of 310 and 316 fish from Guam and Pohnpei, respectively, female maturation could be estimated at 145 mm FL and Males at 178 mm in Guam. However, an L_{50} could not be estimated for the samples in Pohnpei as mature fish were present across the whole size range sampled (from 120 to 263 mm). The authors suggest this species has very early initial development towards maturation.

Spawning aggregations were sampled at 4 different aggregation sites; Big Drop-off, Blue Corner, New Drop-off and Shark City. These aggregations form around the last quarter moon from December to March each year and Both have their spawning during lunar periods of neap tides with midday high tides (Etpison & Colin 2018). These aggregations persist for serval days before swimming out into the blue water far away from the reef for spawning and at this time are heavily predated on by sharks. Despite efforts to witness spawning, this was not confirmed from our observations.

This species was found to have spawning capable gonads all through the year and not related to particular moon phases. As this species are very abundant on Indo-

Pacific coral reefs and from conspicuous aggregations only at certain times of the year, we assume these aggregations do not represent the main mode of spawning for this species, and they likely spawn regularly in pairs or small groups. Although actual spawning has not been witnessed, courtship behaviour in small groups has been observed on the reef crest at the start of the run-out tide close to sunset.

A comparison of length frequencies between sites revealed a very consistent left-hand side of the length frequency distribution (Figure 35B). The male L_{50} value intersects in the range as what is expected from other aggregation formatting species sampled in this study (Figure 6), whereas the female and gender combined estimates are smaller than the smallest fish aggregating. To assess if these aggregations were only from male fish, a close inspection of high-resolution images show both males and females aggregating together which can be determined by males have long filamentous caudal fins (Figure 35A).
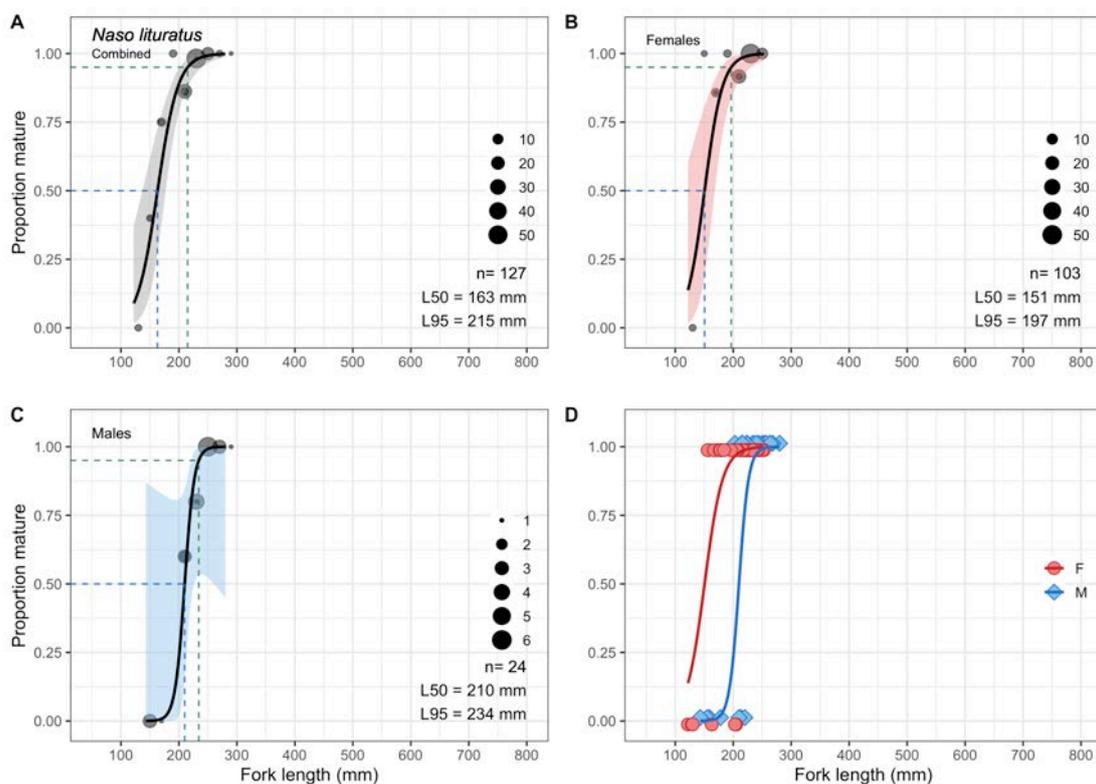
Figure 34. *Naso lituratus* relationships between length and the proportion mature. (A) Gender combined. (B) Female only. (C) Male only. (D) Genders overlaid showing individual samples. Solid line represents the logistic binomial regression and the shaded area represents the 95% confidence intervals. Samples sizes (n) and estimates of L_{50} and L_{95}, are in bottom right-hand corner of each plot.
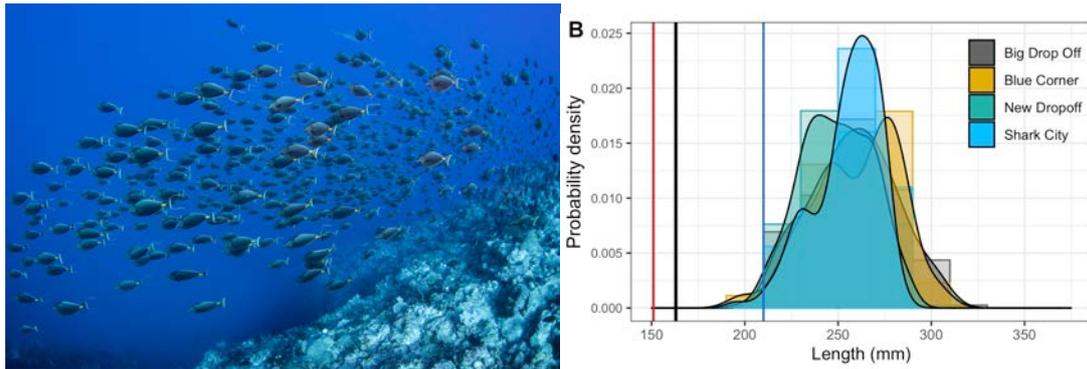
Figure 35. (A) Image of *Naso lituratus* forming a spawning aggregation at New Drop-off. (B) Length frequency comparison between the 4 sites where length measurements were taken. Solid vertical lines indicate the size at maturity (L_{50}) values with combined sexes as black, females as red and males as blue.
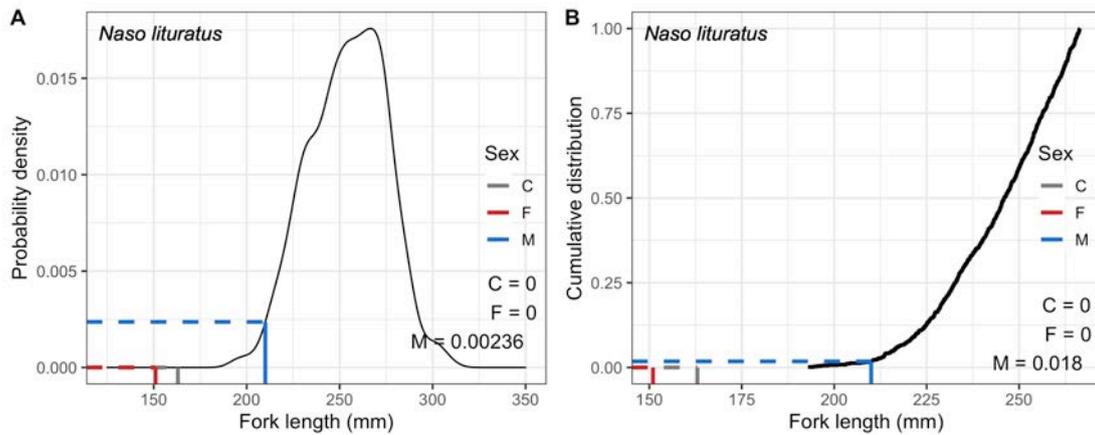
Figure 36. *Naso lituratus* relationships between the spawning aggregation length frequency distribution and the size of maturity (L_{50}) values. (A) Probability density curve and the corresponding y-intercept value that intersects with the maturity values on the x-axis. The probability density value for the gender combined, female and male estimates are displayed in the bottom right of the plot. (B) Cumulative relative frequency plot showing the left-hand side of the length frequency distribution and where the L_{50} values correspond to the proportional cumulative distribution.

Plectropomus areolatus

A total of 114 *Plectropomus areolatus* were sampled for maturity and 494 fish measured from spawning aggregations. The estimates of L_{50} for both sexes combined was 382 mm TL (Figure 37) which was much the same as the female estimate since there were no immature males sampled.

Previous maturity estimates have been derived for this species by several different studies. Firstly, Rhodes et al. (2013) reported a value of 366 mm TL for females in their results text, however closer inspection of their Figure 5 revealed the length at 50% maturity was between 330 and 340 mm, it has been confirmed by the authors that the true value is actually 336 mm. Another recent study in nearby Chuuk state

of the Federated States of Micronesia showed that maturation was even smaller with female fish L_{50} being 302 mm TL and 299 mm for all fish combined (Rhodes et al. 2020). In the Solomon islands, L_{50} was estimated for female fish at two locations; Ghizo where L_{50} was 322 mm and Parara where it was slightly larger at 338 mm (Hughes 2017). Our maturity estimate is significantly higher than from these other studies in nearby locations.

Plectropomus areolatus spawning aggregations form year-round in Palau at certain spawning sites, the two main sites being Ebiil and Ulong Channel. Numbers at the aggregations peak during the 7-month ban grouper fishing from the 1st of April to the 31st October each year and peak numbers have been recorded at Ebiil in June 2019 reaching 1800 fish (Sadovy de Mitcheson et al. 2020). These fish aggregate for a week before the new moon with peak densities normally occurring 3 days before the new moon. Despite focused research on these aggregations for the past two decades (Johannes 1999; Golbuu & Friedlander 2011; Colin et al. 2013; Sadovy de Mitcheson et al. 2020), spawning has not witnessed, but is certain these aggregation events are for spawning with ripe fish with enlarged gonads present at the site during these times along with courtship displays, and we suspect spawning occurs at night in the early hours of the morning. Time-lapse cameras were placed at the Ebiil aggregation site to try and document spawning during the day and at night using red lights outside the visible spectrum of fish, but this was not successful capturing any spawning activity.

This species was the only aggregating fish in this study where we observed groups of immature fish in the aggregation. In June and July 2019 at the Ebiil site, we observed groups (3–50 fish) of small dark-coloured fish moving around the site. These formed a separate peak in length frequency (200–300 mm TL), suggesting that they are not yet sexually mature and may be learning about the site from adults (Sadovy de Mitcheson et al. 2020)

To compare length frequencies between locations and the L_{50} classification scheme used by other researchers, we also sampled two spawning aggregations of this species in Pohnpei, Federated States of Micronesia (2600 km from Palau). In Pohnpei the size at maturity was estimated as 336 mm by Rhodes et al. (2013) in Pohnpei which is 88% of size we estimated in Palau. Sampling took place over 5 days in April 2019 where 262 fish were measured in Pohnpei, and this was compared to 15 days in Palau, where the majority of measurements were from Ebiil and Ulong channel, with a smaller sample size of 82 fish from an aggregation at the northernmost atoll in Palau, Ngeruangel (Figure 38B). The comparison between Palau and Pohnpei revealed aggregating fish were larger in Palau and this was consistently reflected in the relative differences in size at maturity between the locations (Figure 39).
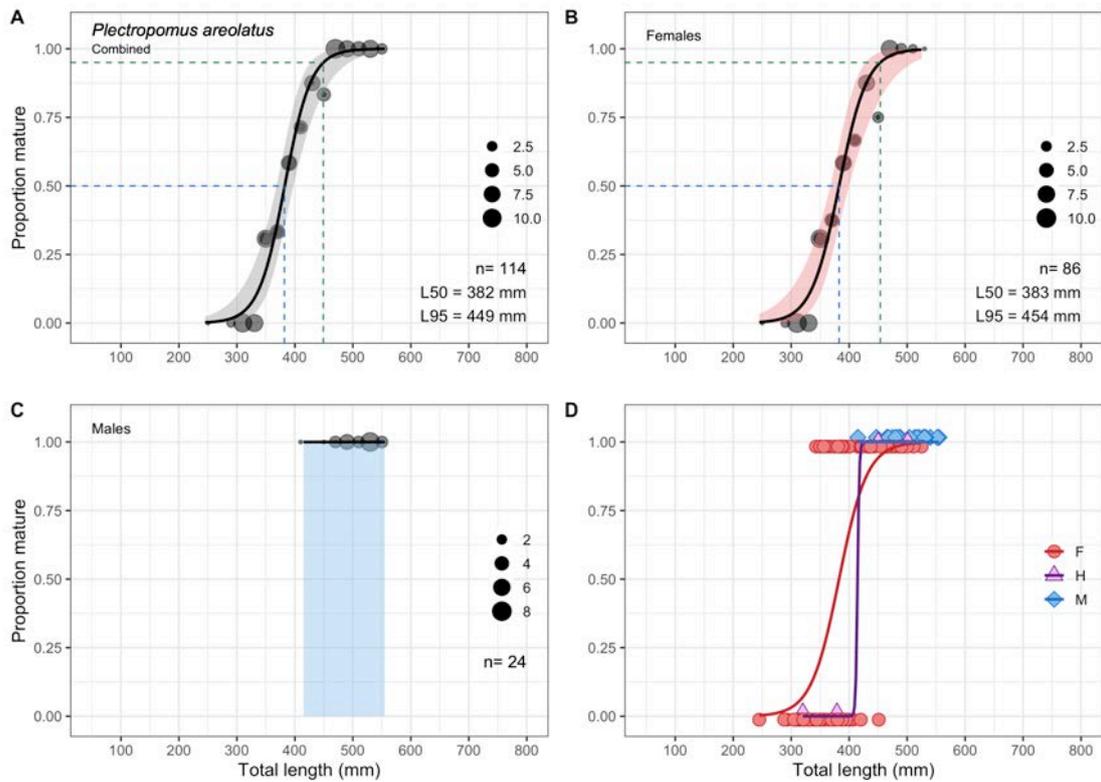
Figure 37. *Plectropomus areolatus* relationships between length and the proportion mature. (A) Gender combined. (B) Female only. (C) Male only. (D) Genders overlaid showing individual samples. Solid line represents the logistic binomial regression and the shaded area represents the 95% confidence intervals. Samples sizes (n) and estimates of L_{50} and L_{95}, are in bottom right-hand corner of each plot.
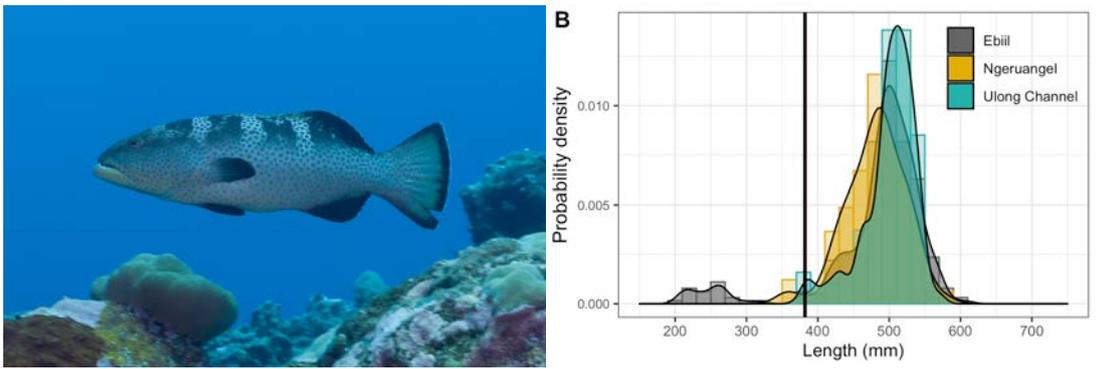
Figure 38. (A) Image of *Plectropomus areolatus* at the spawning aggregation at in Pohnpei. (B) Length frequency comparison between the three sites where length measurements were taken in Palau. Solid vertical lines indicate the size at maturity (L_{50}) values with combined sexes as black and females as red.
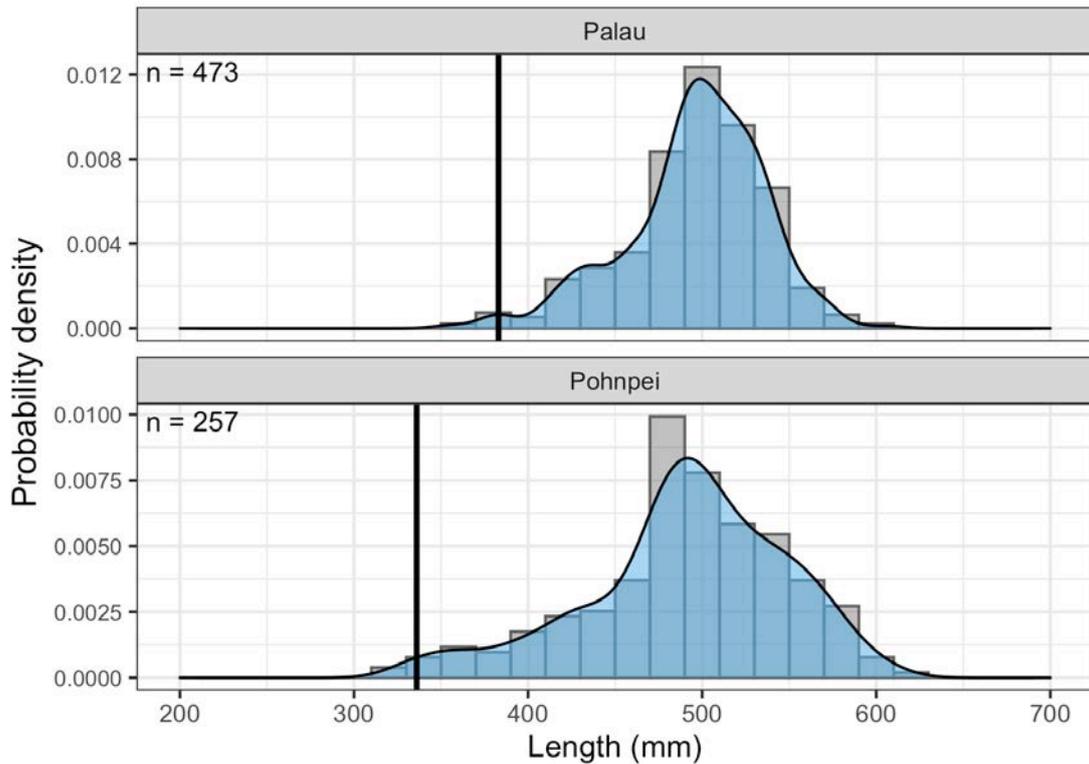
Figure 39. Comparison of *Plectropomus areolatus* length frequencies between Palau and Pohnpei along with their respective L_{50} values as vertical black lines. The presumed immature fish from the Ebiil site in Palau were removed for this comparison.
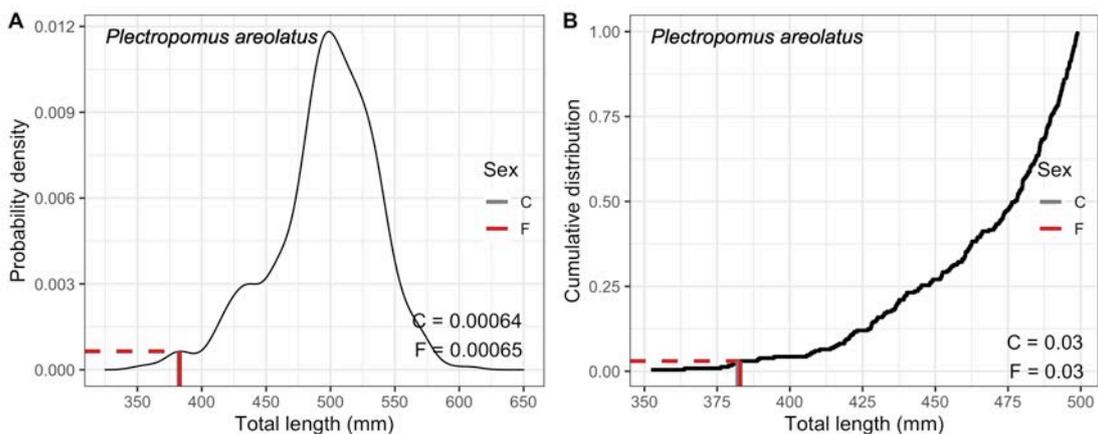
Figure 40. *Plectropomus areolatus* relationships between the spawning aggregation length frequency distribution and the size of maturity (L_{50}) values for Palau. The presumed immature fish from the Ebiil site in Palau were removed for this analysis. (A) Probability density curve and the corresponding y-intercept value that intersects with the maturity values on the x-axis. The probability density value for the gender combined, female estimates are displayed in the bottom right of the plot. (B) Cumulative relative frequency plot showing the left-hand side of the length frequency distribution and where the L_{50} values correspond to the proportional cumulative distribution.

Symphorichthys spilurus

Only 65 *Symphorichthys spilurus* were sampled for maturity, but 1602 were measured from spawning aggregations. The estimates of L_{50} for both sexes combined was 338 mm FL and females matured at a slightly smaller size (330 mm) compared to males (346 mm) (Figure 41). There are no other published maturity estimates for this species.

This species forms the largest known reef fish spawning aggregation in Palau with over 50,000 fish estimated at peak times (Sakaue et al. 2016). These fish aggregate to spawn at the southern promontory of Peleliu, a site well known for spawning aggregations. They begin to aggregate at a site 1-1.5 km from the spawning site around the full moons in February, March and April and commence spawning behaviour on the last quarter moon for a week before the new moon. Smaller aggregations have also been observed in October-November on some years. This species also aggregates to spawn on the north-eastern promontory of the northern lagoon of Palau, a site called Ngerael. We sampled 145 fish from that aggregation but did not observe spawning. Smaller schools have been seen at the Shark City site but were not able to be measured.

We compared the lengths of fish between the Peleliu and Ngerael aggregations to find fish were smaller at Ngerael (Figure 42B). We unsure if this reflects geographic differences in maturity schedules within Palau or it is to do with the fact that these fish were sampled on the new moon in October. It could be that fish have finished spawning for this period and the larger fish have already dispersed from the site leaving smaller fish behind. We also compared survey days in two different years at Peleliu to find very similar size distributions.
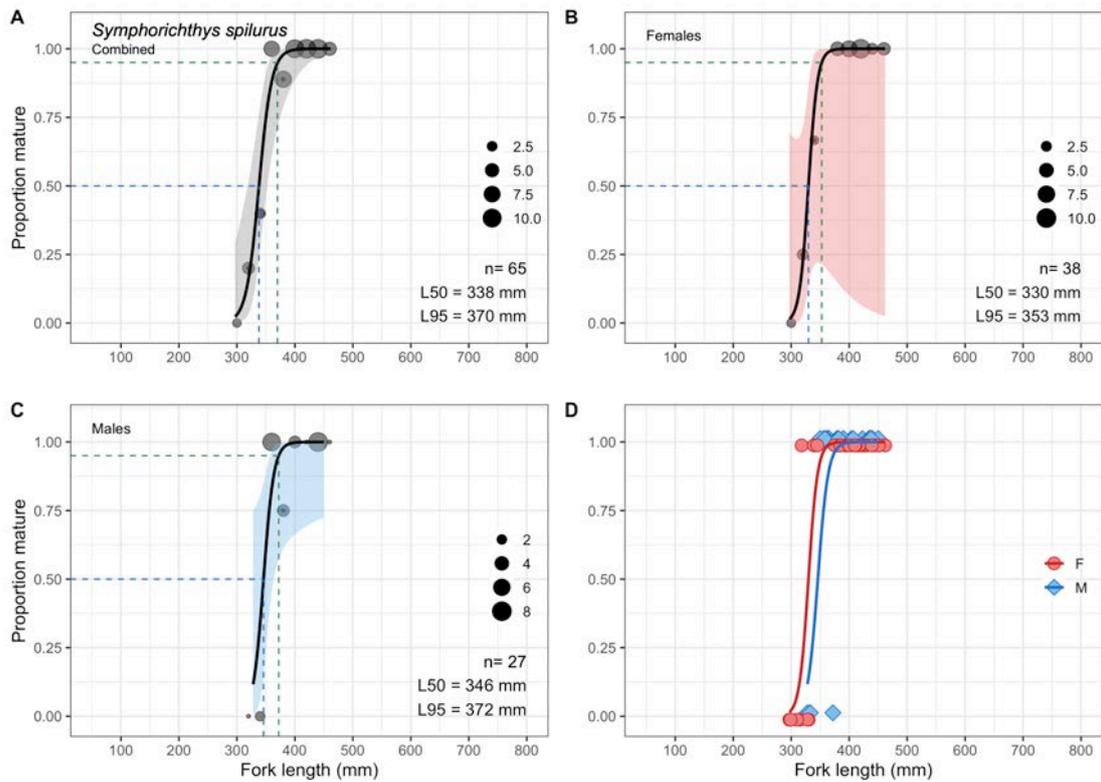
Figure 41. *Symphorichthys spilurus* relationships between length and the proportion mature. (A) Gender combined. (B) Female only. (C) Male only. (D) Genders overlaid showing individual samples. Solid line represents the logistic binomial regression and the shaded area represents the 95% confidence intervals. Samples sizes (n) and estimates of L_{50} and L_{95}, are in bottom right-hand corner of each plot.
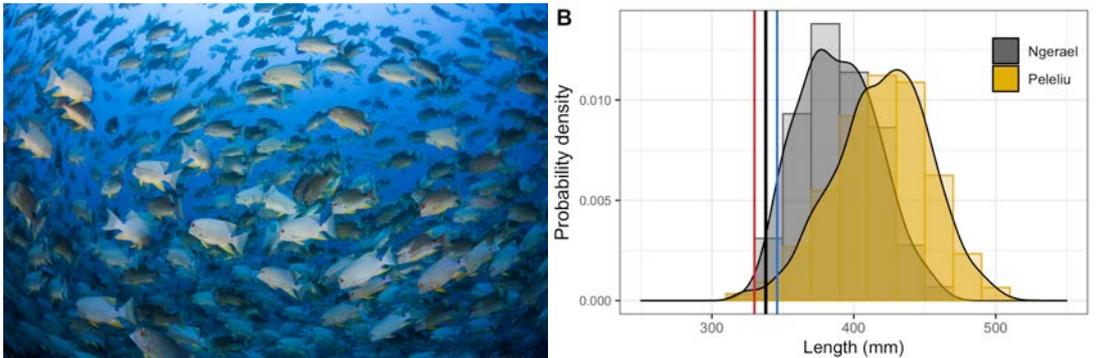
Figure 42. (A) Image of *Symphorichthys spilurus* at the spawning aggregation at Peleliu. (B) Length frequency comparison between aggregation sites from the northern (Ngerael) and southern (Peleliu) tips of the main island group of Palau. Solid vertical lines indicate the size at maturity (L_{50}) values with combined sexes as black and females as red.
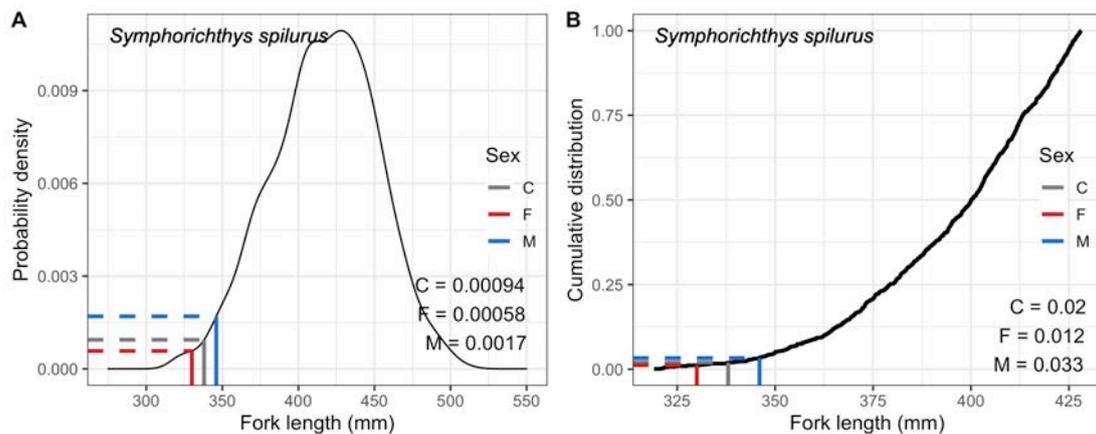
Figure 43. *Symphorichthys spilurus* relationships between the spawning aggregation length frequency distribution and the size of maturity (*L*$_{50}$) values for Palau. (A) Probability density curve and the corresponding y-intercept value that intersects with the maturity values on the x-axis. The probability density value for the gender combined, female and male estimates are displayed in the bottom right of the plot. (B) Cumulative relative frequency plot showing the left-hand side of the length frequency distribution and where the *L*$_{50}$ values correspond to the proportional cumulative distribution.

Modelling L$_{50}$ estimates from length frequency distributions

The gender combined estimates of *L*$_{50}$ for each species were compared to their probability density curve from the length frequency distribution and to the cumulative relative frequency (CRF) formed from the size classes on the left-hand side of the histogram leading up to the main modal size. These two distributions can convert the shape of the length frequencies to be comparable across species with different sample sizes. We theoretically expected the size at maturity estimates would coincide between the 25th – 50th percentile CRF values as a proportion of the population reaches maturity. However, in most cases the *L*$_{50}$ estimates were similar to the size of the smallest individuals in spawning aggregations, being approximated by CRF = 0.

As the CRF plot was not useful to provide values below the *L*$_{50}$, we also fitted a probability density function to the length frequency data using a kernel density estimate (with gaussian distribution) which can extrapolate the curve to along the x-axis to a y-intercept of 0. This provides a way to generate standardised probability densities with the coincidence of the *L*$_{50}$ values on the far left of the frequency distribution. The values for where the *L*$_{50}$ lengths coincide with the probability density and CRF curves for individual species are presented in Table 2.

Table 2. Values for where the gender specific L_{50} values coincide with the probability density and CRF curves for individual species

Taxa	Gender	L_{50} (mm)	Probability density	CRF cumulative distribution
	Combined	286	0.00125	0.017
Caranx melampygus	Female	305	0.0044	0.118
	Male	273	0.00028	0
	Combined	109	0	0
Ctenochaetus striatus	Female	108	0	0
	Male	106	0	0
Epinephelus fuscoguttatus	Combined	563	0.00067	0.00775
	Female	563	0.00067	0.00775
Epinephelus polyphekadion	Combined	357	0.00095	0.015
	Female	358	0.00103	0.019
	Combined	251	0.00039	0
Hipposcarus longiceps	Female	250	0.00034	0
	Male	246	0.00015	0
Lethrinus obsoletus	Combined	212	0.00029	0
	Female	222	0.00226	0
Lethrinus olivaceus	Combined	423	0.00020	0
	Female	423	0.00020	0
Lethrinus xanthochilus	Combined	306	0.00173	0.014
	Female	306	0.00173	0.014
	Combined	402	0.00006	0
Lutjanus bohar	Female	422	0.00027	0.005
	Male	384	0	0
	Combined	163	0	0
Naso lituratus	Female	151	0	0
	Male	210	0.00236	0.018
Plectropomus areolatus	Combined	382	0.00064	0.03
	Female	383	0.00065	0.03
	Combined	338	0.00094	0.02
Symphorichthys spilurus	Female	330	0.00058	0.012
	Male	346	0.0017	0.033

The average probability density value for the gender combined L_{50} is 0.00054 and this value along with its with 95% confidence intervals were tested on normally distributed randomly generated list of lengths with a mean of 400 mm and varying numbers of observations (300-1000) and standard deviations (SD;10-50) (Figure 44). It was evident that a greater standard deviation changed the width of the distribution resulting in smaller predicted L_{50} values and larger confidence intervals, whereas the sample size did not notably change the location of the L_{50} estimates.
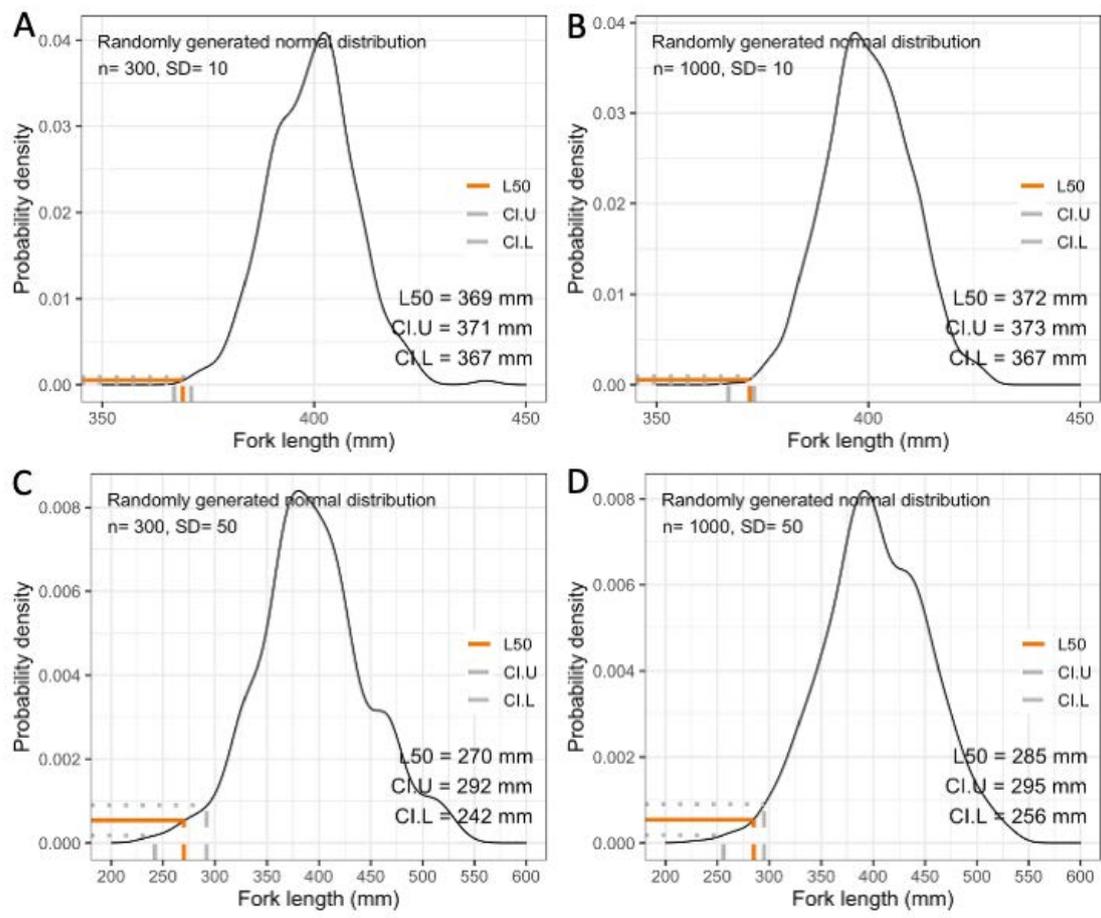
Figure 44. Randomly generated normal distributions with varying numbers of observations (n) and standard deviations (SD). The orange line is the average probability density value that corresponds to the gender combined L_{50} values and their length frequencies from spawning aggregations. Grey lines represent 95% confidence intervals. The text on the bottom right shows the predicted L_{50} and the upper (CI.U) and lower (CI.L) confidence intervals.

Predicting size at maturity for other species that form aggregations

Using the framework developed to estimate L_{50} from an average probability density value, we applied this to 6 species that were filmed in spawning aggregations with stereo-video. These fish species could not be obtained in sufficient numbers to do conventional size at maturity studies though the dissection and interpretation of gonads, due to fish being rarely landed at fish markets or being completely protected from fishing (such as the bumphead parrotfish, *Bolbometopon muricatum* and the humphead wrasse, *Cheilinus undulatus*). The predicted L_{50} values for these six species are presented in Table 3.
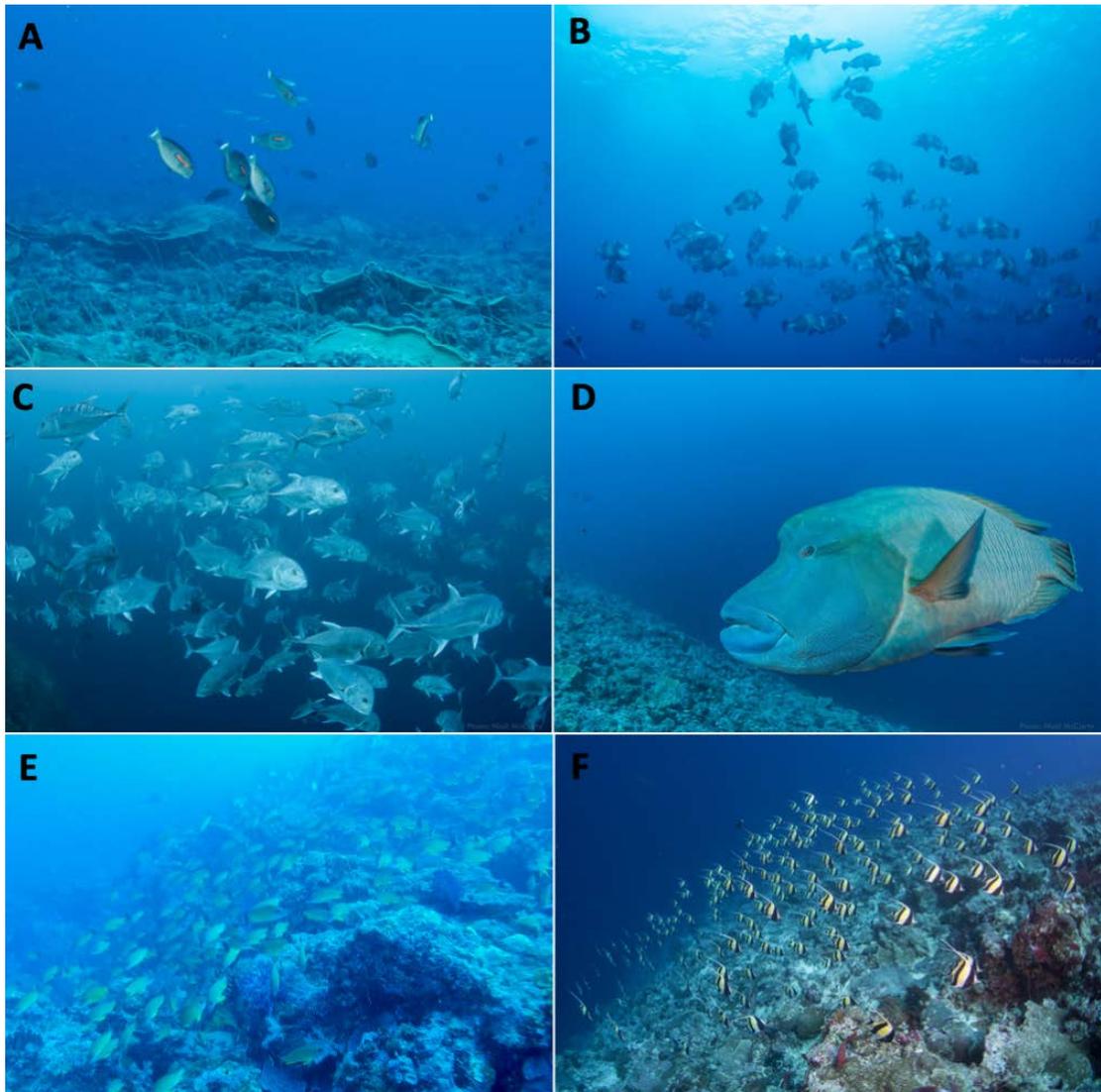
Figure 45. Images of the species that were filmed in aggregations but not biologically sampled for maturity. (A) *Acanthurus olivaceus*, (B) *Bolbometopon muricatum*, (C) *Caranx ignobilis*, (D) *Cheilinus undulatus*, (E) *Lutjanus fulvus*, (F) *Zanclus cornutus.*
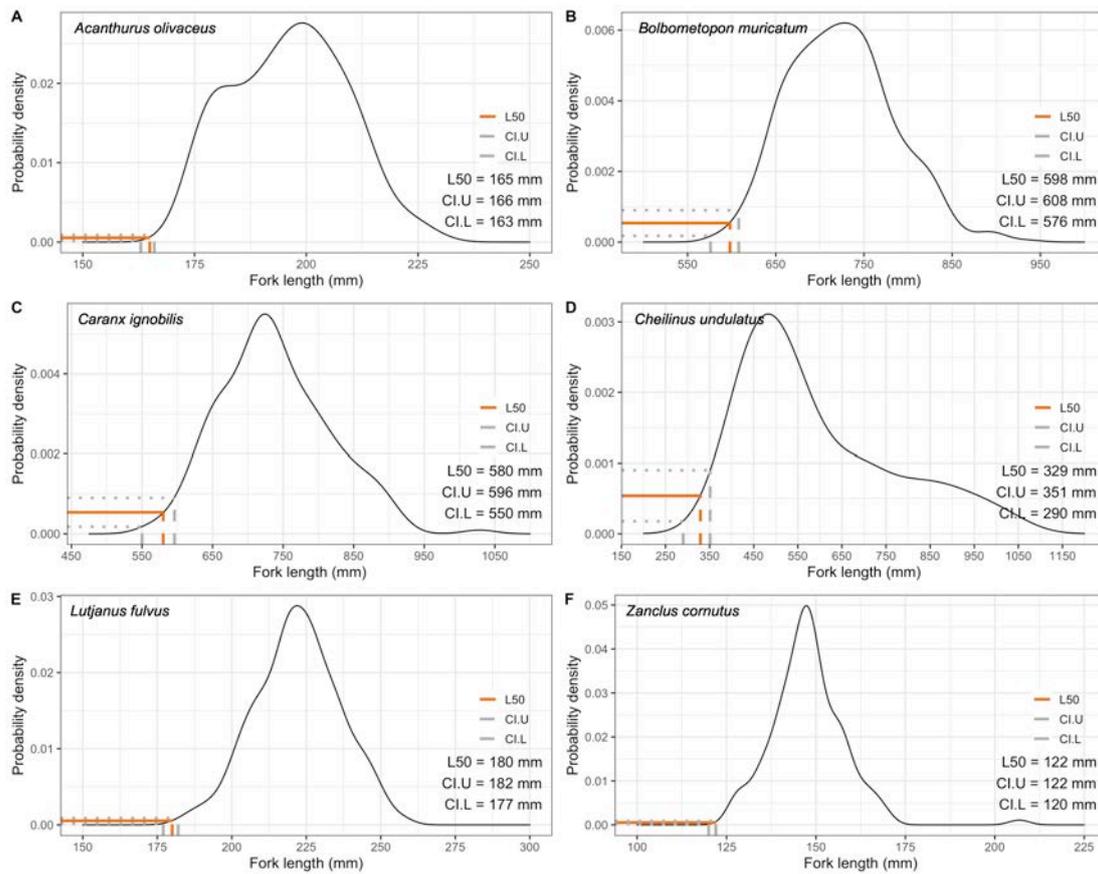
Figure 46. Prediction of L_{50} values for six species measured for length frequency distributions in spawning aggregations. The horizontal orange line is the average probability density value that corresponds to the gender combined L_{50} values and length frequencies from spawning aggregations and the vertical line is where this value intersects the length frequency distribution at a particular length. Grey lines represent 95% confidence intervals. The text on the bottom right shows the predicted L_{50} and the upper (CI.U) and lower (CI.L) confidence intervals.

Table 3. Predicted L_{50} values for six species measured for length frequency distributions in spawning aggregations along with upper and lower 95% confidence intervals.

Taxa	Predicted L_{50} (mm)	upper 95% CI	lower 95% CI
Acanthurus olivaceus	165	166	133
Bolbometopon muricatum	598	608	576
Caranx ignobilis	580	596	550
Cheilinus undulatus	329	351	290
Lutjanus fulvus	180	182	177
Zanclus cornutus	122	122	120

Comparing lengths from spawning aggregation and fishery catches

Comparing the length frequencies from fishery catches in Palau to those measured by stereo-video in aggregations, revealed species specific patterns (Figure 47). Generally, the modal length was larger at aggregations with *Caranx melampygus* and *Ctenochaetus striatus* being exceptions, and for other species both of these length frequencies had similar maximum lengths.

By comparing the catch lengths to the size at maturity, we can determine the percentage of the catch that is immature (Figure 47). Four of these species had more than 20% of the catch being immature. This was highest for *Epinephelus fuscoguttatus* with 78% and for *Lethrinus olivaceus* and *Lutjanus bohar* which had around 40% of the fish landed being caught before they had the chance to reproduce.
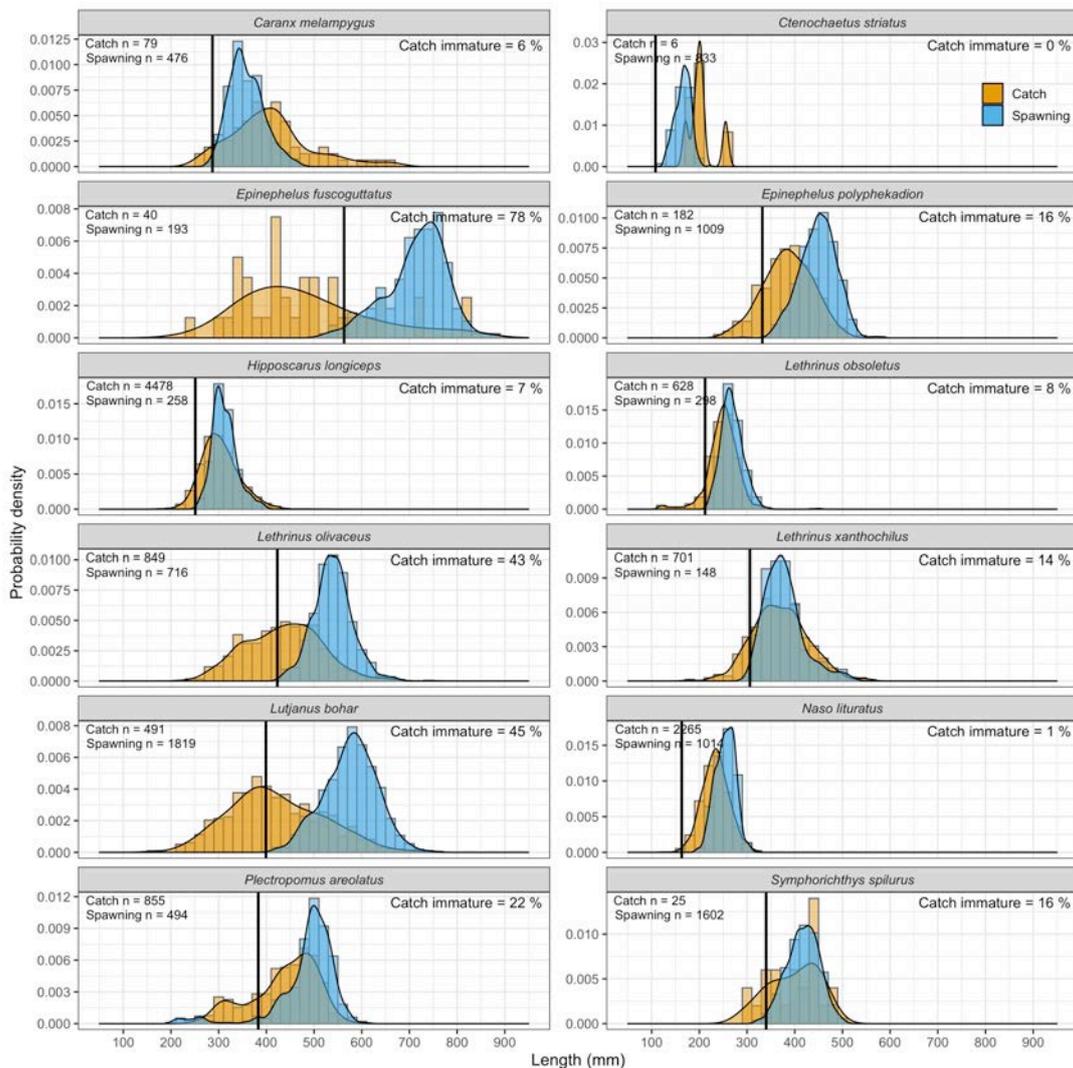
Figure 47. Length frequency distributions for the 12 species sampled with stereo-video at aggregations (blue fill) and the lengths of fish caught and landed in Palau (yellow fill). Solid vertical lines indicate gender combined size at maturity (*L₅₀*) values. Sample sizes (n) of the for the number of fish measured by each technique is in the top left of each plot and the percentage immature in the top right of each plot.

Size limit recommendations

The oldest and simplest form of fishery management is to directly manage size selectivity, this basic prescription has been shown to provide sustainable yields and prevent stock collapse even without other management intervention (Prince & Hordyk 2019). Using a 'rule of thumb' management intervention is important for data-poor fisheries so it can be quickly implemented to halt fishery declines while there is still time. The use of size limits is the simplest way and most effective way to manage the size selectivity of the fishery and by setting minimum size limits between 1.1 – 1.2 x the L_{50}, it can provide decent yields and prevent stock decline (Prince & Hordyk 2019). Under this premise, we provide upper and lower ranges for suggested size limits in Palau (Table 5). As there are many different species, it may be more practical to group fish into relatively few size limit classes for easier community participation and enforcement, as has been recommend in Palau by Prince (unpublished report to TNC in 2016) and in Fiji (Prince et al. 2018).

By predicting the L_{50} for six species that form aggregations that were not sampled for maturity studies we can now also confident about biologically meaningful size limits, but it should be noted that two of these species, the bumphead parrotfish, *Bolbometopon muricatum* and the humphead wrasse, *Cheilinus undulatus*, are protected from fishing and we recommend keeping this ban as they are highly susceptible to fishing pressure. This is especially true for *Cheilinus undulatus* where females mature at a small size (330 mm), but later change sex to males at a significantly greater size and attain a maximum size of at least 1. 2 m. As this is a highly sought after species, with unmanaged fishing pressure there is a real risk of overfishing males which could lead to stock collapse as has happened in other parts of the world, resulting in this species being classified as Endangered by the IUCN (Russell 2014). Other species listed here may not need size limits since they are infrequency targeted and this includes *Ctenochaetus striatus, Symphorichthys spilurus, Acanthurus olivaceus, Lutjanus fulvus* and *Zanclus cornutus.* However, all other species listed would benefit from the implementation of size limits.

Table 5. Suggested size limits for the 18 species measured with stereo-video in aggregations. Size limits based on multiplying the L_{50} by a minimum of 1.1x and a maximum of 1.2x which should preserve at least 20% SPR. The length type refers to measuring the fish by fork length (FL) or the total length (TL) when caudal fin is not forked.

Taxa	Length type	L_{50} (mm)	Lower range (mm)	Upper range (mm)	Median size limit (mm)	Median size limit (inches)
Caranx melampygus	FL	286	315	343	329	13
Ctenochaetus striatus	FL	109	120	131	125	5
Epinephelus fuscoguttatus	TL	563	619	676	647	25
Epinephelus polyphekadion	TL	357	393	428	411	16
Hipposcarus longiceps	FL	251	276	301	289	11
Lethrinus obsoletus	FL	212	233	254	244	10
Lethrinus olivaceus	FL	423	465	508	486	19
Lethrinus xanthochilus	FL	306	337	367	352	14
Lutjanus bohar	FL	402	442	482	462	18
Naso lituratus	FL	163	179	196	187	7
Plectropomus areolatus	TL	382	420	458	439	17
Symphorichthys spilurus	FL	338	372	406	389	15
Acanthurus olivaceus	FL	165	182	198	190	7
Bolbometopon muricatum	TL	598	658	718	688	27
Caranx ignobilis	FL	580	638	696	667	26
Cheilinus undulatus	TL	329	362	395	378	15
Lutjanus fulvus	FL	180	198	216	207	8
Zanclus cornutus	FL	122	134	146	140	6

Conclusion

This study proved it is possible to use of diver operated stereo-video at fish spawning aggregations to estimate size at maturity and therefore provides a fishery-independent alternative to the dissection and examination of fish gonads. If fish spawning aggregations are accessible for sampling with stereo-video, this new method can be used to cost-effectively and accurately estimate size at maturity. These maturity values can be used to recommend biologically meaningful size limits or run data-poor stock assessments if there is adequate size frequency data on fishery catches.

This newly developed technique also has application for expanding surveys across other coral reef locations to cost effectively compare the variation in life-history values across geographic gradients using a standardized technique. The main limiting factor for LB-SPR assessments and size limit recommendation throughout other regions in the world is the lack of locally derived size at maturity data. We realise this is a massive task to estimate these values for the hundreds of different species targeted by subsistence fisheries, and by providing this new shortcut method it could be of use in places where known spawning aggregations are accessible for diving. Although this method in itself will not be able to cover the

majority of species caught by fishing, it is possible that a prediction factor could be used if different species vary their size at maturity in a consistent ratio at different locations. For example, *Plectropomus areolatus* matured at a size 12% smaller in Pohnpei compared to Palau and based on L_{50} values another grouper *Epinephelus polyphekadion* matured at a size 8% smaller. However, on the other hand, we found *Hipposcarus longiceps* to mature at a size 23% larger in Pohnpei compared to Palau. Further research is clearly needed in order to understand relative differences in size at maturity between geographic locations and species, and we believe this fishery-independent method would be a useful tool for this purpose.

Another by-product of this work was the acquisition of fish otoliths for the 1325 fish sampled. As there is a lack of published life-history ratios for many coral reef species, and it is hoped that these otoliths could be used for future studies to develop age-based life-history ratios which are used as parameters for LB-SPR assessments. As only one of the four parameters used for assessments required can be calculated from maturity data (L_m), the remaining three; M (the rate of natural mortality), k (the von Bertalanffy growth co-efficient) and $L\infty$ (asymptotic size), require age-based studies on growth and mortality. With the addition of age-based results for these species, it would be possible to focus the same framework to correlate the coincidence of the probability density curve to the next most important value for LB-SPR assessments that is likely to vary between locations, the asymptotic length (L_∞).

Acknowledgements

References

Andrew NL, Béné C, Hall SJ, Allison EH, Heck S, Ratner BD. 2007. Diagnosis and management of small-scale fisheries in developing countries. Fish and Fisheries **8**:227–240.

Brown-Peterson NJ, Wyanski DM, Saborido-Rey F, Macewicz BJ, Lowerre-Barbieri SK. 2011. A standardized terminology for describing reproductive development in fishes. Marine and Coastal Fisheries **3**:52–70.

Caillart B, Harmelin-Vivien ML, Galzin R, Morize E. 1994. Reef Fish Communities and Fishery Yields of Tikehau Atoll (Tuamotu Archipelago French Polynesia). Atoll Research Bulletin.

Colin P. 2012a. Timing and Location of Aggregation and Spawning in Reef Fishes. Pages 117–158 in Y. Sadovy de Mitcheson and P. Colin, editors. Reef fish spawning aggregations: biology, research and management. Springer.

Colin P. 2012b. Longnose Parrotfish – Hipposcarus longiceps. Pages 496–502 in Y. Sadovy de Mitcheson and P. Colin, editors. Reef fish spawning aggregations: biology, research and management. Springer.

Colin P. 2012c. Bigeye Trevally – Caranx sexfasciatus with Notes on Other Jacks (Carangidae). Pages 507–513 in Y. Sadovy de Mitcheson and P. L. Colin, editors. Reef fish spawning aggregations: biology, research and management. Springer.

Colin PL. 2010. Aggregation and spawning of the humphead wrasse *Cheilinus undulatus* (Pisces: Labridae): general aspects of spawning behaviour. Journal of Fish Biology **76**:987–1007.

Colin PL, Sadovy de Mitcheson Y, Donaldson TJ. 2013. Grouper spawning aggregations: Be careful what you measure and how you measure it: A rebuttal of Golbuu and Friedlander (2011). Estuarine, Coastal and Shelf Science **123**:1–6.

DeMartini EE, Langston RC, Eble JA. 2014. Spawning seasonality and body sizes at sexual maturity in the bluespine unicornfish, Naso unicornis (Acanthuridae). Ichthyological Research **61**:243–251.

Domeier ML, Colin PL. 1997. Tropical reef fish spawning aggregations: defined and reviewed. Bulletin of Marine Science **60**:698–726.

Erisman B, Heyman W, Kobara S, Ezer T, Pittman S, Aburto-Oropeza O, Nemeth RS. 2015. Fish spawning aggregations: where well-placed management actions can yield big benefits for fisheries and conservation. Fish and Fisheries **18**:128–144.

Etpison MT, Colin PL. 2018. Blue Water Spawning by Moorish Idols and Orangespine Surgeonfish in Palau: Is it a "Suicide Mission"? **23**:16.

Flores A, Wiff R, Diaz E. 2015. Using the gonadosomatic index to estimate the maturity ogive: application to Chilean hake (Merluccius gayi gayi). ICES Journal of Marine Science **72**:508–514.

Goetze JS, Bond T, McLean DL, Saunders BJ, Langlois TJ, Lindfield S, Fullwood LAF, Driessen D, Shedrawi G, Harvey ES. 2019. A field and video analysis

guide for diver operated stereo-video. Methods in Ecology and Evolution **10**:1083–1090.

Golbuu Y, Friedlander AM. 2011. Spatial and temporal characteristics of grouper spawning aggregations in marine protected areas in Palau, western Micronesia. Estuarine, Coastal and Shelf Science **92**:223–231.

Harvey E, Fletcher D, Shortis M. 2002. Estimation of reef fish length by divers and by stereo-video: a first comparison of the accuracy and precision in the field on living fish under operational conditions. Fisheries Research **57**:255–265.

Harvey E, Goetze J, McLaren B, Langlois T, Shortis M. 2010. Influence of range, angle of view, image resolution and image compression on underwater stereo-video measurements: high-definition and broadcast-resolution video cameras compared. Marine Technology Society Journal **44**:75–85.

Hordyk A, Ono K, Valencia S, Loneragan N, Prince J. 2015. A novel length-based empirical estimation method of spawning potential ratio (SPR), and tests of its performance, for small-scale, data-poor fisheries. ICES Journal of Marine Science **72**:217–231.

Hughes AT. 2017. Demographic and reproductive characteristics of the squaretail coralgrouper (Plectropomus areolatus) in Solomon Islands. James Cook University, Townsville, QLD, Australia.

Johannes RE. 1981. Words of the lagoon: fishing and marine lore in the Palau district of Micronesia. University of California Press, Los Angeles.

Johannes RE. 1999. Spawning aggregations of groupers (Serranidae) in Palau. The Nature Conservancy.

Junquera S, Román E, Morgan J, Sainza M, Ramilo G. 2003. Time scale of ovarian maturation in Greenland halibut (Reinhardtius hippoglossoides, Walbaum). ICES Journal of Marine Science **60**:767–773. Oxford Academic.

Lindfield S. 2017. Palau's reef fisheries: changes in size and spawning potential from past to present. Technical Report. Coral Reef Research Foundation, Palau.

Lindfield SJ, Harvey ES, McIlwain JL, Halford AR. 2014. Silent fish surveys: bubble-free diving highlights inaccuracies associated with SCUBA-based surveys in heavily fished areas. Methods in Ecology and Evolution **5**:1061–1069.

Longenecker K, Langston R, Bolick H, Kondio U. 2013. Rapid reproductive analysis and length–weight relation for blacktail snapper, utjanus fulvus; (actinopterygii: perciformes: lutjanidae), from a remote village in papua new guinea. Acta Ichthyologica Et Piscatoria **43**:51–55.

Longenecker K, Langston R, Bolick H, Kondio U, Mulrooney M. 2014. Six-Year Baseline Information: Size Structure and Reproduction of Exploited Reef Fishes Before Establishing a Management Plan at Kamiali Wildlife Management Area, Papua New Guinea:91.

Loubens G. 1980. Biologie de quelques espèces de Poissons du lagon neo-Calédonien II. Sexualité et reproduction:32.

Mapleston A, Currey LM, Williams AJ, Pears R, Simpfendorfer CA, Penny AL, Tobin A, Welch D. 2009. Comparative biology of key inter-reefal serranid species on the Great Barrier Reef. Project Milestone Report to the Marine and Tropical Sciences Research Facility. Reef and Rainforest Research Centre Limited, Cairns (55 pp.).

Marriott RJ, Jarvis NDC, Adams DJ, Gallash AE, Norriss J, Newman SJ. 2010. Maturation and sexual ontogeny in the spangled emperor Lethrinus nebulosus. Journal of Fish Biology **76**:1396–1414.

Marriott RJ, Mapstone BD, Begg GA. 2007. Age-specific demographic parameters, and their implications for management of the red bass, Lutjanus bohar (Forsskal 1775): A large, long-lived reef fish. Fisheries Research **83**:204–215.

Moore B, Rechelluul P, Victor S, Secretariat of the Pacific Community. 2015. Creel survey and demographic assessments of coastal finfish fisheries of southern Palau, September 2014.

Murphy MD, Taylor RG. 1990. Reproduction, growth, and mortality of red drum Sciaenops ocellatus in Florida waters. Fishery Bulletin **88**:531-542.

Nadon MO, Ault JS, Williams ID, Smith SG, DiNardo GT. 2015. Length-Based Assessment of Coral Reef Fish Populations in the Main and Northwestern Hawaiian Islands. PLOS ONE **10**:e0133960.

Ochavillo D, Tofaeono S, Sabater M, Trip EL. 2011. Population structure of Ctenochaetus striatus (Acanthuridae) in Tutuila, American Samoa: The use of size-at-age data in multi-scale population size surveys. Fisheries Research **107**:14–21.

Ogle D, Wheeler P, Dinno A. 2020. FSA: Fisheries Stock Analysis. R package version 0.8.30. Available from https://github.com/droglenc/FSA.

Pears RJ, Choat JH, Mapstone BD, Begg GA. 2006. Demography of a large grouper, Epinephelus fuscoguttatus, from Australia's Great Barrier Reef: implications for fishery management. Marine Ecology Progress Series **307**:259–272.

Prince J, Hordyk A. 2019. What to do when you have almost nothing: A simple quantitative prescription for managing extremely data-poor fisheries. Fish and Fisheries **20**:224–238.

Prince J, Hordyk A, Valencia SR, Loneragan N, Sainsbury K. 2015a. Revisiting the concept of Beverton-–Holt life-history invariants with the aim of informing data-poor fisheries assessment. ICES Journal of Marine Science **72**:194–203. Oxford Academic.

Prince J, Smith A, Raffe M, Seeto S, Higgs J. 2020. Spawning potential surveys in Solomon Islands' Western Province:11.

Prince J, Victor S, Kloulchad V, Hordyk A. 2015b. Length based SPR assessment of eleven Indo-Pacific coral reef fish populations in Palau. Fisheries Research **171**:42–58.

Prince JD et al. 2018. Developing a system of sustainable minimum size limits for Fiji:10.

R Core Team. 2020. R: A language and environment for statistical computing. R Foundation for Statistical Computing, Vienna, Austria. Available from http://www.R-project.org/.

Rhodes KL, Baremore IE, Taylor BM, Cuetos-Bueno J, Hernandez D. 2020. Aligning fisheries management with life history in two commercially important groupers in Chuuk, Federated States of Micronesia. Aquatic Conservation: Marine and Freshwater Ecosystems:aqc.3452.

Rhodes KL, Nemeth RS, Kadison E, Joseph E. 2014. Spatial, temporal, and environmental dynamics of a multi-species epinephelid spawning aggregation in Pohnpei, Micronesia. Coral Reefs:1–11.

Rhodes KL, Taylor BM, McIlwain JL. 2011. Detailed demographic analysis of an Epinephelus polyphekadion spawning aggregation and fishery. Marine Ecology Progress Series **421**:183–198.

Rhodes KL, Taylor BM, Wichilmel CB, Joseph E, Hamilton RJ, Almany GR. 2013. Reproductive biology of squaretail coralgrouper Plectropomus areolatus using age-based techniques. Journal of fish biology **82**:1333–1350.

Robertson DR, Ackerman JL, Choat JH, Posada JM, Pitt J. 2005. Ocean surgeonfish Acanthurus bahianus. I. The geography of demography. Marine Ecology Progress Series **295**:229–244.

Russell M. 2014. *Cheilinus undulatus*. Available from www.iucnredlist.org (accessed July 29, 2014).

Sadovy de Mitcheson Y, Colin P, Sakaue J. 2012. Lutjanus fulvus – Blacktail Snapper with Notes on Other Species of Atlantic and Indo-Pacific Snappers (Lutjanidae). Pages 458–468 in Y. Sadovy de Mitcheson and P. L. Colin, editors. Reef fish spawning aggregations: biology, research and management. Springer.

Sadovy de Mitcheson Y, Colin PL, Lindfield SJ, Bukurrou A. 2020. A Decade of Monitoring an Indo-Pacific Grouper Spawning Aggregation: Benefits of Protection and Importance of Survey Design. Frontiers in Marine Science **7**. Frontiers. Available from https://www.frontiersin.org/articles/10.3389/fmars.2020.571878/full (accessed November 18, 2020).

Sadovy Y. 2007. Report on current status and exploitation history of reef fish spawning aggregations in Palau. Western Pacific Fishery Survey Series: Society for the Conservation of Reef Fish Aggregations **3**:40.

Sakaue J, Akino H, Endo M, Ida H, Asahida T. 2016. Temporal and spatial site sharing during spawning in snappers Symphorichthys spilurus and Lutjanus bohar (Pisces: Perciformes: Lutjanidae) in waters around Peleliu island, Palau. Zoological Studies **55**:1–15.

Shortis M, Harvey E, Abdo D. 2009. A review of underwater stereo-image measurement for marine biology and ecology applications. Oceanography and Marine Biology: An Annual Review **47**:257–292.

Sudekum AE, Parrish JD, Radtke RL, Ralston S. 1991. Life history and ecology of large jacks in undisturbed, shallow, oceanic communities. Fishery Bulletin **89**:493–513.

Taylor BM. 2010. Life-history and per-recruit assessment of *Lethrinus obsoletus* from Guam. Technical Report 128. University of Guam Marine Laboratory, Mangilao.

Taylor BM, Choat JH. 2014. Comparative demography of commercially important parrotfish species from Micronesia. Journal of Fish Biology **84**:383–402.

Taylor BM, Choat JH, DeMartini EE, Hoey AS, Marshell A, Priest MA, Rhodes KL, Meekan MG. 2019. Demographic plasticity facilitates ecological and

economic resilience in a commercially important reef fish. Journal of Animal Ecology **88**:1888–1900.

Taylor BM, Cruz E. 2017. Age-based and reproductive biology of the Pacific Longnose Parrotfish Hipposcarus longiceps from Guam. PeerJ **5**:e4079.

Taylor BM, Gourley J, Trianni MS. 2016. Age, growth, reproductive biology and spawning periodicity of the forktail rabbitfish (Siganus argenteus) from the Mariana Islands. Marine and Freshwater Research **68**:1088–1097.

Taylor BM, Oyafuso ZS, Pardee CB, Ochavillo D, Newman SJ. 2018. Comparative demography of commercially-harvested snappers and an emperor from American Samoa. PeerJ **6**:e5069.

Taylor BM, Oyafuso ZS, Trianni MS. 2017. Life history of the orange-striped emperor Lethrinus obsoletus from the Mariana Islands. Ichthyological Research **64**:423–432. Springer.

Taylor BM, Rhodes KL, Marshell A, McIlwain JL. 2014. Age-based demographic and reproductive assessment of orangespine Naso lituratus and bluespine Naso unicornis unicornfishes. Journal of Fish Biology **85**:901–916.

Trip EL, Choat JH, Wilson DT, Robertson DR. 2008. Inter-oceanic analysis of demographic variation in a widely distributed Indo-Pacific coral reef fish. Marine Ecology Progress Series **373**:97–109.

Vitale F, Svedäng H, Cardinale M. 2006. Histological analysis invalidates macroscopically determined maturity ogives of the Kattegat cod (Gadus morhua) and suggests new proxies for estimating maturity status of individual fish. ICES Journal of Marine Science **63**:485–492.

West G. 1990. Methods of assessing ovarian development in fishes: a review. Marine and Freshwater Research **41**:199–222.

Wright A, Dalzell PJ, Richards AH. 1986. Some aspects of the biology of the red bass, Lutjanus bohar (Forsskal), from the Tigak Islands, Papua New Guinea. Journal of fish biology **28**:533–544.